



**THE DETERMINATION OF ISOTOPE PRODUCTION OF
HEAVY ELEMENTS WITH DIFFERENT MODELS**

Begard Kareem ABBAS

Master's Thesis

Physics department

Thesis Advisor: Prof. Dr. İskender DEMİRKOL

2017

All rights reserved

Republic of Turkey
BİNGÖL UNIVERSITY
INSTITUTE OF SCIENCE

**THE DETERMINATION OF ISOTOPE PRODUCTION
OF HEAVY ELEMENTS WITH DIFFERENT MODELS**

MASTER'S THESIS

Begard Kareem ABBAS

Institute Department : PHYSICS

Thesis Advisor : Prof. Dr. İskender DEMİRKOL

May 2017

PREFACE

To begin with, I thank (Allah) for his blessing who made me able to complete and perform this study with success. I would like to thank my supervisor, Prof. Dr. İskender DEMİRKOL who does not spare his help and knowledge and gives the necessary support for the completion of my studies, during the course of the thesis.

I would like to thank Bingöl University Rector, the manager and staff of central laboratory for their support for the thesis work. I must express my very profound gratitude to my mother and members of my family for providing me with unfailing support and continuous encouragement throughout my years of study and through the process of researching and writing this thesis.

I must express my very profound gratitude to my parents and members of my family for providing me with unfailing support and continuous encouragement throughout my years of study and through the process of researching and writing this thesis. Finally, I am thankful to my colleagues and all others friends for their help and encouragement.

Begard Kareem ABBAS

Bingöl 2017

CONTENT

PREFACE.....	ii
CONTENT.....	iii
LIST OF SYMBOLS AND ABBREVIATIONS.....	vi
LIST OF FIGURES.....	viii
LIST OF TABLES.....	xi
ÖZET.....	xii
ABSTRACT.....	xiv
1. INTRODUCTION.....	1
2. LITERATURE REVIEW.....	3
3. MATERIAL AND METHOD.....	7
3.1. Spallation.....	7
3.1.1. Spallation reaction.....	7
3.1.2. Spallation target.....	8
3.2. Accelerator driven system (ADS).....	8
3.2.1. History of accelerators.....	9
3.2.2. Developmet of accelerators.....	9
3.3. Accelerators.....	10
3.3.1. Tandem Van de Graff electrostatic accelerators.....	10
3.3.2. Linear accelerators (Linac).....	10
3.4. Total reaction cross section.....	11
3.5. Production of residual nuclides.....	11
3.6. Light charged particle Production.....	12
3.7. Production of residual nuclei in reverse kinematics.....	13
3.8. Codes and high energy models.....	14

3.9. Method	15
3.10. The nuclear model.....	15
3.10.1. Pre-Equilibrium reactions.....	16
3.10.2. Common characteristics of pre-Equilibrium models.....	17
3.10.3. Full exciton model.....	17
3.10.4. Hybrid model.....	18
3.10.5. Geometry dependents hybrid model.....	19
3.10.6. Cascade exciton model.....	20
3.11. Evaporation model.....	21
4. RESULT AND DISCUSSION.....	22
4.1. Calculation method	22
4.2. CEM03 Computar program	22
4.3. ALICE / ASH Computar program	23
4.4. $p+ {}_{83}\text{Bi}^{209}$ Reaction.....	25
4.4.1. ${}_{83}\text{Bi}^{204-209}$ the product ion resulting from the reaction of $p+{}_{83}\text{Bi}^{209}$	25
4.4.2. ${}_{84}\text{Po}^{204-210}$ the product resulting from the reaction of $p+{}_{83}\text{Bi}^{209}$	26
4.4.3. ${}_{82}\text{Pb}^{198-208}$ the product resulting from the reaction of $p+{}_{83}\text{Bi}^{209}$	27
4.4.4. ${}_{82}\text{Pb}^{198-208}$ the product resulting from the reaction of $p+{}_{83}\text{Bi}^{209}$	29
4.4.5. ${}_{81}\text{Tl}^{195-205}$ the product resulting from the reaction of $p+{}_{83}\text{Bi}^{209}$	30
4.4.6. ${}_{82}\text{Pb}^{194-208}$ the product resulting from the reaction of $p+{}_{83}\text{Bi}^{209}$	31
4.4.7. ${}_{84}\text{Po}^{197-209}$ the product resulting from the reaction of $p+{}_{83}\text{Bi}^{209}$	33
4.4.8. ${}_{81}\text{Tl}^{191-208}$ the product resulting from the reaction of $p+{}_{83}\text{Bi}^{209}$	34
4.4.9. ${}_{82}\text{Pb}^{192-208}$ the product resulting from the reaction of $p+{}_{83}\text{Bi}^{209}$	36
4.4.10. ${}_{84}\text{Po}^{195-209}$ the product resulting from the reaction of $p+{}_{83}\text{Bi}^{209}$	37
4.4.11. ${}_{82}\text{Pb}^{192-208}$ the product resulting from the reaction of $p+{}_{83}\text{Bi}^{209}$	39
4.4.12. ${}_{84}\text{Po}^{195-209}$ the product resulting from the reaction of $p+{}_{83}\text{Bi}^{209}$	40
4.4.13. ${}_{82}\text{Pb}^{190-208}$ the product resulting from the reaction of $p+{}_{83}\text{Bi}^{209}$	42
4.4.14. ${}_{81}\text{Tl}^{189-208}$ the product resulting from the reaction of $p+{}_{83}\text{Bi}^{209}$	43
4.4.15. ${}_{84}\text{Po}^{194-209}$ the product resulting from the reaction of $p+{}_{83}\text{Bi}^{209}$	45
4.5. $p+ {}_{74}\text{W}^{184}$ Reaction.....	47
4.5.1. ${}_{75}\text{Re}^{179-185}$ the product resulting from the reaction of $p+{}_{74}\text{W}^{184}$	47
4.5.2. ${}_{74}\text{W}^{179-184}$ the product resulting from the reaction of $p+{}_{74}\text{W}^{184}$	48
4.5.3. ${}_{73}\text{Ta}^{173-183}$ the product resulting from the reaction of $p+ {}_{74}\text{W}^{184}$	49

4.5.4. ${}_{75}\text{Re}^{175-184}$ the product resulting from the reaction of $p+{}_{74}\text{W}^{184}$	51
4.5.5. ${}_{72}\text{Hf}^{169-180}$ the product resulting from the reaction of $p+{}_{74}\text{W}^{184}$	52
4.5.6. ${}_{73}\text{Ta}^{169-183}$ the product resulting from the reaction of $p+{}_{74}\text{W}^{184}$	53
4.5.7. ${}_{75}\text{Re}^{171-184}$ the product resulting from the reaction of $p+{}_{74}\text{W}^{184}$	55
4.5.8. ${}_{72}\text{Hf}^{165-180}$ the product resulting from the reaction of $p+{}_{74}\text{W}^{184}$	56
4.5.9. ${}_{73}\text{Ta}^{167-183}$ the product resulting from the reaction of $p+{}_{74}\text{W}^{184}$	58
4.5.10. ${}_{75}\text{Re}^{171-184}$ the product resulting from the reaction of $p+{}_{74}\text{W}^{184}$	59
4.5.11. ${}_{72}\text{Hf}^{165-180}$ the product resulting from the reaction of $p+{}_{74}\text{W}^{184}$	61
4.5.12. ${}_{72}\text{Hf}^{163-183}$ the product resulting from the reaction of $p+{}_{74}\text{W}$	62
4.5.13. ${}_{73}\text{Ta}^{165-183}$ the product resulting from the reaction of $p+{}_{74}\text{W}^{184}$	64
4.5.14. ${}_{75}\text{Re}^{171-184}$ the product resulting from the reaction of $p+{}_{74}\text{W}^{184}$	66
5. CONCLUSION.....	68
REFERENCES.....	69
CURRICULUM VITAE.....	74

LIST OF SYMBOLS

ADS	: Accelerator driven system
DC	: Direct current
Line Ac	: Linear accelerators
CEM	: Cascade exciton modele
LAHET	: Monte carlo code for the transport and interaction of nucleons
RAL	: Rutherford Appleton laboratory
INC	: Intra nuclear cascade
GEANT4	: Details of the object-oriented
GeV	: Giga electron volt
MeV	: Mega electron volt
eV	: Electron volt
RF	: Radio frequency
E	: Energy
P	: Momentum
ΔP	: Momentum change
μA	: Micro ampere
τ	: Torsion
σ	: Sigma (Effect section)
ε	: Epsilon

e^-	:	Electron
e^+	:	Positron
p	:	Proton
n	:	Neutron
σ_R	:	Reaction cross section
λ_C	:	Propagation speed
W	:	Tungsten
Bi	:	Bismuth
Z	:	Atomic number
A	:	Mass number
H_0	:	Model hamiltonian

LIST OF FIGURES

Figure 3.1.	Spallation reaction.....	8
Figure 4.1.	Mass number (A) cross sections obtained for isotope of ^{83}Bi at reaction $p+ ^{83}\text{Bi}^{209}$; $E_p=50$ MeV energy. Calculations have been made with CEM03 and ALICE/ASH code.....	26
Figure 4.2.	Mass number (A) cross sections obtained for isotope of ^{84}Po at reaction $p+ ^{83}\text{Bi}^{209}$; $E_p=50$ MeV energy. Calculations have been made with CEM03 and ALICE/ASH and PCROS code.....	27
Figure 4.3.	Mass number (A) cross sections obtained for isotope of ^{82}Pb at reaction $p+ ^{83}\text{Bi}^{209}$; $E_p=100$ MeV energy. Calculations have been made with CEM03 and ALICE/ASH code.....	28
Figure 4.4.	Mass number (A) cross sections obtained for isotope of ^{82}Pb at reaction $p+ ^{83}\text{Bi}^{209}$; $E_p=100$ MeV energy. Calculations have been made with CEM03 and ALICE/ASH code and experimental data.....	30
Figure 4.5.	Mass number (A) cross sections obtained for isotope of ^{81}Tl at reaction $p+ ^{83}\text{Bi}^{209}$; $E_p=150$ MeV energy. Calculations have been made with CEM03 and ALICE/ASH code.....	31
Figure 4.6.	Mass number (A) cross sections obtained for isotope of ^{82}Pb at reaction $p+ ^{83}\text{Bi}^{209}$; $E_p=150$ MeV energy. Calculations have been made with CEM03 and ALICE/ASH code.....	32
Figure 4.7.	Mass number (A) cross sections obtained for isotope of ^{84}Po at reaction $p+ ^{83}\text{Bi}^{209}$; $E_p=150$ MeV energy. Calculations have been made with CEM03 and ALICE/ASH code.....	34
Figure 4.8.	Mass number (A) cross sections obtained for isotope of ^{81}Tl at reaction $p+ ^{83}\text{Bi}^{209}$; $E_p=200$ MeV energy. Calculations have been made with CEM03 and ALICE/ASH code.....	35

Figure 4.9.	Mass number (A) cross sections obtained for isotope of $_{82}\text{Pb}$ at reaction $p+_{83}\text{Bi}^{209}$; $E_p=200$ MeV energy. Calculations have been made with CEM03 and ALICE/ASH code.....	37
Figure 4.10.	Mass number (A) cross sections obtained for isotope of $_{84}\text{Po}$ at reaction $p+_{83}\text{Bi}^{209}$; $E_p=200$ MeV energy. Calculations have been made with CEM03 and ALICE/ASH code.....	38
Figure 4.11.	Mass number (A) cross sections obtained for isotope of $_{82}\text{Pb}$ at reaction $p+_{83}\text{Bi}^{209}$; $E_p=200$ MeV energy. Calculations have been made with CEM03 and ALICE/ASH code.....	40
Figure 4.12.	Mass number (A) cross sections obtained for isotope of $_{84}\text{Po}$ at reaction $p+_{83}\text{Bi}^{209}$; $E_p=200$ MeV energy. Calculations have been made with CEM03 and ALICE/ASH code.....	41
Figure 4.13.	Mass number (A) cross sections obtained for isotope of $_{82}\text{Pb}$ at reaction $p+_{83}\text{Bi}^{209}$; $E_p=250$ MeV energy. Calculations have been made with CEM03 and ALICE/ASH code.....	43
Figure 4.14.	Mass number (A) cross sections obtained for isotope of $_{81}\text{Tl}$ at reaction $p+_{83}\text{Bi}^{209}$; $E_p=250$ MeV energy. Calculations have been made with CEM03 and ALICE/ASH code.....	44
Figure 4.15.	Mass number (A) cross sections obtained for isotope of $_{84}\text{Po}$ at reaction $p+_{83}\text{Bi}^{209}$; $E_p=250$ MeV energy. Calculations have been made with CEM03 and ALICE/ASH code.....	46
Figure 4.16.	Mass number (A) cross sections obtained for isotope of $_{75}\text{Re}$ at reaction $p+_{74}\text{W}^{184}$; $E_p=50$ MeV energy. Calculations have been made with CEM03 and ALICE/ASH and PCROS code.....	48
Figure 4.17.	Mass number (A) cross sections obtained for isotope of $_{74}\text{W}$ at reaction $p+_{74}\text{W}^{184}$; $E_p=50$ MeV energy. Calculations have been made with CEM03 and ALICE/ASH and PCROS code.....	49
Figure 4.18.	Mass number (A) cross sections obtained for isotope of $_{73}\text{Ta}$ at reaction $p+_{74}\text{W}^{184}$; $E_p=100$ MeV energy. Calculations have been made with CEM03 and ALICE/ASH code.....	50
Figure 4.19.	Mass number (A) cross sections obtained for isotope of $_{75}\text{Re}$ at reaction $p+_{74}\text{W}^{184}$; $E_p=100$ MeV energy. Calculations have been made with CEM03 and ALICE/ASH code.....	51
Figure 4.20.	Mass number (A) cross sections obtained for isotope of $_{72}\text{Hf}$ at reaction	

	p+ ${}_{74}\text{W}^{184}$; $E_p=150$ MeV energy. Calculations have been made with CEM03 and ALICE/ASH code.....	53
Figure 4.21.	Mass number (A) cross sections obtained for isotope of ${}_{73}\text{Ta}$ at reaction p+ ${}_{74}\text{W}^{184}$; $E_p=150$ MeV energy. Calculations have been made with CEM03 and ALICE/ASH code.....	54
Figure 4.22.	Mass number (A) cross sections obtained for isotope of ${}_{75}\text{Re}$ at reaction p+ ${}_{74}\text{W}^{184}$; $E_p=150$ MeV energy. Calculations have been made with CEM03 and ALICE/ASH code.....	56
Figure 4.23.	Mass number (A) cross sections obtained for isotope of ${}_{72}\text{Hf}$ at reaction p+ ${}_{74}\text{W}^{184}$; $E_p=200$ MeV energy. Calculations have been made CEM03 with ALICE/ASH code.....	57
Figure 4.24.	Mass number (A) cross sections obtained for isotope of ${}_{73}\text{Ta}$ at reaction p+ ${}_{74}\text{W}^{184}$; $E_p=200$ MeV energy. Calculations have been made with CEM03 and ALICE/ASH code.....	59
Figure 4.25.	Mass number (A) cross sections obtained for isotope of ${}_{75}\text{Re}$ at reaction p+ ${}_{74}\text{W}^{184}$; $E_p=200$ MeV energy. Calculations have been made with CEM03 and ALICE/ASH code.....	60
Figure 4.26.	Mass number (A) cross sections obtained for isotope of ${}_{72}\text{Hf}$ at reaction p+ ${}_{74}\text{W}^{184}$; $E_p=200$ MeV energy. Calculations have been made with CEM03 and ALICE/ASH code.....	62
Figure 4.27.	Mass number (A) cross sections obtained for isotope of ${}_{72}\text{Hf}$ at reaction p+ ${}_{74}\text{W}^{184}$; $E_p=250$ MeV energy. Calculations have been made with CEM03 and ALICE/ASH code.....	64
Figure 4.28.	Mass number (A) cross sections obtained for isotope of ${}_{73}\text{Ta}$ at reaction p+ ${}_{74}\text{W}^{184}$; $E_p=250$ MeV energy. Calculations have been made with CEM03 and ALICE/ASH code.....	65
Figure 4.29.	Mass number (A) cross sections obtained for isotope of ${}_{75}\text{Re}$ at reaction p+ ${}_{74}\text{W}^{184}$; $E_p=250$ Mev energy. Calculations have been made with CEM03 and ALICE/ASH code.....	67

LIST OF TABLES

Table 4.1.	Mass number (A) cross sections obtained for isotope of ^{83}Bi at reaction $p+ ^{83}\text{Bi}^{209}$; $E_p=50$ MeV energy. Calculations have been made with CEM03 and ALICE/ASH and PCROS code	26
Table 4.2.	Mass number (A) cross sections obtained for isotope of ^{84}Po at reaction $p+ ^{83}\text{Bi}^{209}$; $E_p=50$ MeV energy. Calculations have been made with CEM03 and ALICE/ASH and PCROS code	27
Table 4.3.	Mass number (A) cross sections obtained for isotope of ^{82}Pb at reaction $p+ ^{83}\text{Bi}^{209}$; $E_p=100$ MeV energy. Calculations have been made with CEM03 and ALICE/ASH code and experimental data.....	28
Table 4.4.	Mass number (A) cross sections obtained for isotope of ^{82}Pb at reaction $p+ ^{83}\text{Bi}^{209}$; $E_p=100$ MeV energy. Calculations have been made with CEM03 and ALICE/ASH code and experimental data.....	29
Table 4.5.	Mass number (A) cross sections obtained for isotope of ^{81}Tl at reaction $p+ ^{83}\text{Bi}^{209}$; $E_p=150$ MeV energy. Calculations have been made with CEM03 and ALICE/ASH code	32
Table 4.6.	Mass number (A) cross sections obtained for isotope of ^{82}Pb at reaction $p+ ^{83}\text{Bi}^{209}$; $E_p=150$ MeV energy. Calculations have been made with CEM03 and ALICE/ASH code	33
Table 4.7.	Mass number (A) cross sections obtained for isotope of ^{84}Po at reaction $p+ ^{83}\text{Bi}^{209}$; $E_p=150$ MeV energy. Calculations have been made with CEM03 and ALICE/ASH code	33
Table 4.8.	Mass number (A) cross sections obtained for isotope of ^{81}Tl at reaction $p+ ^{83}\text{Bi}^{209}$; $E_p=200$ MeV energy. Calculations have been made with CEM03 and ALICE/ASH code	35

Table 4.9.	Mass number (A) cross sections obtained for isotope of ^{82}Pb at reaction $p+ {}_{83}\text{Bi}^{209}$; $E_p=200$ MeV energy. Calculations have been made with CEM03 and ALICE/ASH code	36
Table 4.10.	Mass number (A) cross sections obtained for isotope of ^{84}Po at reaction $p+ {}_{83}\text{Bi}^{209}$; $E_p=200$ MeV energy. Calculations have been made with CEM03 and ALICE/ASH code	38
Table 4.11.	Mass number (A) cross sections obtained for isotope of ^{82}Pb at reaction $p+ {}_{83}\text{Bi}^{209}$; $E_p=200$ MeV energy. Calculations have been made with CEM03 and ALICE/ASH code	39
Table 4.12.	Mass number (A) cross sections obtained for isotope of ^{84}Po at reaction $p+ {}_{83}\text{Bi}^{209}$; $E_p=200$ MeV energy. Calculations have been made with CEM03 and ALICE/ASH code	41
Table 4.13.	Mass number (A) cross sections obtained for isotope of ^{82}Pb at reaction $p+ {}_{83}\text{Bi}^{209}$; $E_p=250$ MeV energy. Calculations have been made with CEM03 and ALICE/ASH code	42
Table 4.14.	Mass number (A) cross sections obtained for isotope of ^{81}Tl at reaction $p+ {}_{83}\text{Bi}^{209}$; $E_p=250$ MeV energy. Calculations have been made with CEM03 and ALICE/ASH code	44
Table 4.15.	Mass number (A) cross sections obtained for isotope of ^{84}Po at reaction $p+ {}_{83}\text{Bi}^{209}$; $E_p=250$ MeV energy. Calculations have been made with CEM03 and ALICE/ASH code	45
Table 4.16.	Mass number (A) cross sections obtained for isotope of ^{75}Re at reaction $p+ {}_{74}\text{W}^{184}$; $E_p=50$ MeV energy. Calculations have been made with CEM03 and ALICE/ASH and PCROS code	47
Table 4.17.	Mass number (A) cross sections obtained for isotope of ^{74}W at reaction $p+ {}_{74}\text{W}^{184}$; $E_p=50$ MeV energy. Calculations have been made with CEM03 and ALICE / ASH and PCROS code	49
Table 4.18.	Mass number (A) cross sections obtained for isotope of ^{73}Ta at reaction $p+ {}_{74}\text{W}^{184}$; $E_p=100$ MeV energy. Calculations have been made with CEM03 and ALICE/ASH code	50
Table 4.19.	Mass number (A) cross sections obtained for isotope of ^{75}Re at reaction $p+ {}_{74}\text{W}^{184}$; $E_p=100$ MeV energy. Calculations have been made with CEM03 and ALICE/ASH code	51
Table 4.20.	Mass number (A) cross sections obtained for isotope of ^{72}Hf at reaction	

	p+ ${}_{74}\text{W}^{184}$; $E_p=150$ MeV energy. Calculations have been made with CEM03 and ALICE/ASH code.....	52
Table 4.21.	Mass number (A) cross sections obtained for isotope of ${}_{73}\text{Ta}$ at reaction p+ ${}_{74}\text{W}^{184}$; $E_p=150$ MeV energy. Calculations have been made with CEM03 and ALICE/ASH code.....	54
Table 4.22.	Mass number (A) cross sections obtained for isotope of ${}_{75}\text{Re}$ at reaction p+ ${}_{74}\text{W}^{184}$; $E_p=150$ MeV energy. Calculations have been made with CEM03 and ALICE/ASH code.....	55
Table 4.23.	Mass number (A) cross sections obtained for isotope of ${}_{72}\text{Hf}$ at reaction p+ ${}_{74}\text{W}^{184}$; $E_p=200$ MeV energy. Calculations have been made with CEM03 and ALICE/ASH code.....	57
Table 4.24.	Mass number (A) cross sections obtained for isotope of ${}_{73}\text{Ta}$ at reaction p+ ${}_{74}\text{W}^{184}$; $E_p=200$ MeV energy. Calculations have been made with CEM03 and ALICE/ASH code.....	58
Table 4.25.	Mass number (A) cross sections obtained for isotope of ${}_{75}\text{Re}$ at reaction p+ ${}_{74}\text{W}^{184}$; $E_p=200$ MeV energy. Calculations have been made with CEM03 and ALICE/ASH code.....	60
Table 4.26.	Mass number (A) cross sections obtained for isotope of ${}_{72}\text{Hf}$ at reaction p+ ${}_{74}\text{W}^{184}$; $E_p=200$ MeV energy. Calculations have been made with CEM03 and ALICE/ASH code and experimental data.....	61
Table 4.27.	Mass number (A) cross sections obtained for isotope of ${}_{72}\text{Hf}$ at reaction p+ ${}_{74}\text{W}^{184}$; $E_p=250$ MeV energy. Calculations have been made with CEM03 and ALICE/ASH code.....	63
Table 4.28.	Mass number (A) cross sections obtained for isotope of ${}_{73}\text{Ta}$ at reaction p+ ${}_{74}\text{W}^{184}$; $E_p=250$ MeV energy. Calculations have been made with CEM03 and ALICE / ASH code.....	65
Table 4.29.	Mass number (A) cross sections obtained for isotope of ${}_{75}\text{Re}$ at reaction p+ ${}_{74}\text{W}^{184}$; $E_p=250$ MeV energy. Calculations have been made with CEM03 and ALICE / ASH code.....	66

FARKLI MODELLERDE AĞIR ÖĞELERİN İZOTOP ÜRETİMİNİN BELİRLENMESİ

ÖZET

Bu çalışmada $p + {}_{74}\text{W}^{184}$ ve $p + {}_{83}\text{Bi}^{209}$ reaksiyonlarındaki artık nüklidlerin üretim taser kesitleri hesaplanmıştır. Proton ışınları 30-500 MeV enerji aralığına sahiptir. Hesaplamalar, denge öncesi, İntra nükleer Kaskat Model ve Cascade Exciton Modeli kullanılarak yapılmıştır. İzotopların oluşum tesir kesitleri hesanlanmıştır. Hesaplamalar CEM03 ve ALICE / ASH ve PCROS programları kullanılarak yapılmıştır. Sonuçlar mevcut deney verileri ile karşılaştırılmıştır. $p + {}_{74}\text{W}^{184}$ ve $p + {}_{83}\text{Bi}^{209}$ reaksiyonu için ${}_{82}\text{Pb}$, ${}_{81}\text{Ti}$, ${}_{84}\text{Po}$, ${}_{73}\text{Ta}$, ${}_{75}\text{Re}$ ve ${}_{72}\text{Hf}$ ve elementlerinin çeşitli izotopları farklı proton enerjilerde elde edilmiştir.

Anahtar Kelimeler: nötron üretimi, hızlandırıcılar, hızlı Proton, spallation, izotop üretimi.

THE DETERMINATION OF ISOTOPE PRODUCTION OF HEAVY ELEMENTS WITH DIFFERENT MODELS

ABSTRACT

In this study, the fragmentation production cross sections of residual nuclides in the reactions $p + {}_{74}\text{W}^{184}$, and $p + {}_{83}\text{Bi}^{209}$ have been calculated. Proton beams have an energy range of 30-500 MeV. Calculations have been made using pre-equilibrium, Intra-nuclear Cascade Model and Cascade Exciton Model. The formation cross sections of the isotopes are calculated. Calculations have been made using CEM03 and ALICE / ASH and PCROS programs. The results have been compared with the current experimental data. The different isotopes of ${}_{82}\text{Pb}$, ${}_{81}\text{Ti}$, ${}_{84}\text{Po}$, ${}_{73}\text{Ta}$, ${}_{75}\text{Re}$ and ${}_{72}\text{Hf}$ and their elements have been obtained at different proton energies for $p + {}_{74}\text{W}^{184}$ and $p + {}_{83}\text{Bi}^{209}$ reactions.

Key words: neutron production, accelerators, rapid Proton, spallation, isotope production.

1. INTRODUCTION

Until very recently, all our knowledge on the spin-off sections of isotopes of heavy residues from spallation reactions of high energy protons with heavy on radiological methods and mass spectrometry cores. These techniques have given access to the remains of a long life only and therefore have been identified mainly accumulated revenue, resulting from the beta decay of the initial reaction products. Instead of using previous techniques, it has become possible to have access to all primary waste produced by using inverse kinematics throwing liquid hydrogen with heavy ions relativity.

The reaction products are identified in flight in atomic number and in mass using a recoil separator. In addition to identifying the cross production sectors, this technique is also able to give information on the kinematics of the reaction and the speed of the reaction products. Gained reactions fragmentation of much attention recently because of its importance in technical applications. They can, for example, fragmentation shell in the relative energies as one of the main production method has been proposed. Reliable information about the production sectors through individual isotopes in hardware ISOL-type, a method used widely for the production of the radioactive beam can also be obtained by the inverse movement science experiments. One reason for the discrepancy between the experimental data and models is the lack of empirical data. It was difficult to compare the systematic model calculations with experimental data available for the analysis of physical reasons for the shortcomings in the models. The project started in GSI to determine the production sectors across the remains of a 0.1 MB, which is aimed at the accuracy of 10%, reaction fragmentation of 0.8 GeV or 1 GeV protons and 2 GeV deuterons on the target material heavier than gold, lead, and uranium using kinematics inverse. The spin-off of production sections and kinesiology width, measured in the reactions of 0.8 thousand GeV 197 au with protons and heavy products and the products of interaction in the fission (Benlliure 1998).

These reports work to complete the production of isotopes sectors across all elements of titanium ($Z = 22$) to lead ($Z = 82$) measured in inverse kinematics spallation reaction of 1 GeV protons with lead. In addition to, distributions were the measured speed of all isotopes produced, and give important information about the participants in the production reaction mechanism. It has already been considered as part of the current work data for the cross sections of production and kinesiology of heavy residues (Wlazlo et al. 2000).

For every atomic nucleus made consist of a collection of neutron and protons, subatomic particles (However, the hydrogen, which consists of the single proton). Protons with a positive electrical charge, the number in the nucleus is characteristic of each element. Example, the nucleus carbon atoms are always six protons, the oxygen eight. Cascade Exciton Model (CEM) is another calculation method used to calculate the pre-equilibrium calculations of the reactions between the non-energetic particle and the target nucleus. carry out exciton processing of the target particle of the particle sent to the target. Then, this emerging nuclear system begins to emit particles until it reaches a statistical balance (Sarar et al. 2009).

2. LITERATURE REVIEW

(Demirkol et al. 2003) reactions fragmentation has attracted more attention recently due to technical applications as sources of intense neutron reactors subcritical accelerator-driven or spallation neutron source.

(Geissel et al. 1995) studied in the next generation of radioactive beam facilities, shell model in the relative energies be one of the most important means of production.

(Benlliure et al. (1998) studied the production relative peripheral nuclear nucleus of great artistic importance in several aspects of the collision revenue.

(Wlazlo et al. 2000) precision modeling to estimate the cross sections of the remains of the production is still needed now technical applications performance. This can be attributed in large part to the absence of complete distributions of all isotope-producing, which have been limit the models.

(Gudima et al. 1983) studied that the reactions a nucleus-nucleus within the scope of the average power is still to attract a lot of attention, they represent an opportunity to investigate the emissions of particulate matter of balance.

(Barashenkov and Toneev 1972) studied that at the top of the energies of many of the features of the nuclear reactions well to some extent, reproduced within the cascade model into the nucleus.

(Mashnik et al. 2006) it is dealt with later relax nuclear excitement in terms of the exciton, and a form of decay before the balance, which includes a description of the balance of evaporation, the third phase of the reaction (Bertini 1972) Is there a strong way to calculate the reactions is the nucleus of Marne with complex cores over the years evolved. This is the method of the waterfall into the nucleus followed by evaporation.

In this approach, the continuous shifts of high-energy particles and deal with the case of ($E \geq 100$ MeV) on the nucleus as a two-step process. The first step is fast fission cascade, have been described the reaction by a chain reaction of particles individual particles occur within the nucleus. The second is the evaporation of excited molecules remaining after the core chain. In this way, generally Monte Carlo calculation techniques employed.

(Summerer et al. 1990) studied that the formula parameters EPAX cross sections of goals shell fragmentation of measuring the production of high-energy ranging from $A = 40$ and $A = 232$. We can see that these standards give a great deal of public distribution of production in the department.

(De Jong et al. 1998) studied that the shell fragments near the distribution of the remaining count on the ratio of the proton to a neutron shell affected.

(Enqvist et al. 2001) studied that compared with cross sections calculated and experimental fragmentation of the remains as a function of the mass loss to 208 bullets (1 GeV / nucleon) + P reaction. Experimental data transfer.

(Benlliure et al. 1998) studied that the production relative peripheral nuclear nucleolus of great artistic importance in several aspects of the collision revenue.

(Brohm and Schmidt 1994) studied that the FP correction factor, that is, the probability of survival ion completely stripped after passing the layers of material in the target area in S2, decide as a function of the nuclear charge using the procedure described.

(Prael and Lichtenstein 1989) studied that compared to the year, our distribution, and measurement of isotopic distributions of selected items with LAHET code.

(Bertini 1969) implementation of the results of the parameters of each Silberberg others. As shown solid line, and the code to predict because of the line LAHET account. And intermittently using a cascade into the nucleus.

(Gloris et al. 2001) reliable cross-sections for the production of the remaining radionuclides of medium strength and proton reactions caused by neutron ADS is necessary to calculate the radioactive inventory of the target particles from building materials and surrounding

material. The production is the view of the remaining radionuclides of protons GeV goals in thick or large modeling complex that you need to follow. In detail chains between states and within the nuclear program, and the production of primary and secondary particles and transport. Spectra of primary and secondary particles strongly depend on radioactive materials, as well as on the geometry and depth inside the target. For modeling radionuclide inventories have been sufficient as the first to be rounded neutron cross sections up to 200 MeV. The expected annual production measurements resulting from the remaining neutrons between 30 and 180 MeV. Reactions caused by proton and one that needs to complete functions excitement up to the energy of the primary beam. The latter are of recent work our cooperation to the most relevant target elements.

(Chadwick 1999) studied that the description semi-classic in three stages. In the first stage is divided (INC) target in the spherical parts of the nuclear potential and the nucleolus with various neutron and proton number density. The sampling phase of the particles uniformly tracked using Monte Carlo techniques either to describe his movement toward the target or within broker a complex system space.

(Weisskopf 1937) statistical theory of emission of particles from the nuclei of the remaining came after the INC have been originally developed by Weisskopf. This model assumes complete energy balance by the emission of particles, and re-excitation energies between successive evaporation emissions budget. As a result, the angular distribution of emitted particles isotropic.

(Wlazlo et al. 2000) studies that these reports work to complete the production of isotopes sectors across all elements of titanium ($Z = 22$) to lead ($Z = 82$) the inverse- kinematics fragmentation measured the reaction of 1 GeV protons with lead. In addition, distributions were the measured speed of all isotopes produced, giving a critical information on the to participate in the production reaction mechanism. It has already been considered as part of the current work data for the cross sections of production and kinesiology of heavy residues in Wlazlo.

(Yildirm 2009) studied that the some of the oscillator core target group of the cross-section of neutron reaction of protons produced in the reaction of the tax courts inputs and calculate the theoretical spectrum and investigated by comparison with experimental data that have been published.

(Demirkol 2003) studied that in the Gazi University, "power amplifier design of the proton-neutron production of heavy elements in the incident on"Ph.D. thesis formulation. In this study, which has already been compared to theoretical and experimental data.



3. MATERIAL AND METHOD

3.1. Spallation

3.1.1. Spallation Reaction

The main difference between sub-critical particle accelerator driven systems (ADS) and a conventional reactor is the presence of high-energy proton beam and neutron multiplier target regions in the accelerators. High energy (typically > 500 MeV) with a proton beam with a continuous high density of the heavy metal wave, which is sent to the destination. Called at the same time responded spallation act of replies actual act of drawing some of the reactions of the target nuclei or light nuclei. The high energy of the target nucleus based on the interaction with nuclei around a nucleon. Certain of the target nuclei in these two processes, or launchers or dislocation nuclei emitted outside through evaporation. The use of neutrons that result from these nuclei (20 MeV) basic (source) and neutrons in the critical six surrounding court aim to make fission. ADS "fission process about high energy target in order to allow the important spallation six protected to ensure the flow of basic neutron. Spallation proton on the bonds for a number of energy proton beam of neutrons and depends on the material in the core mass. This is due to the cost of determining the power of the accelerator, and therefore ADS "economy neutron is very important for small and medium companies. Fission products subcritical are copied to the court. It contains high levels of radionuclides in nuclear waste spallation neutrons using stable isotopes or short-term very conversion. As a result, the energy proton target material and related studies are to ADS is the number of neutrons in the proton exposed to the importance of the (Genc 2008).

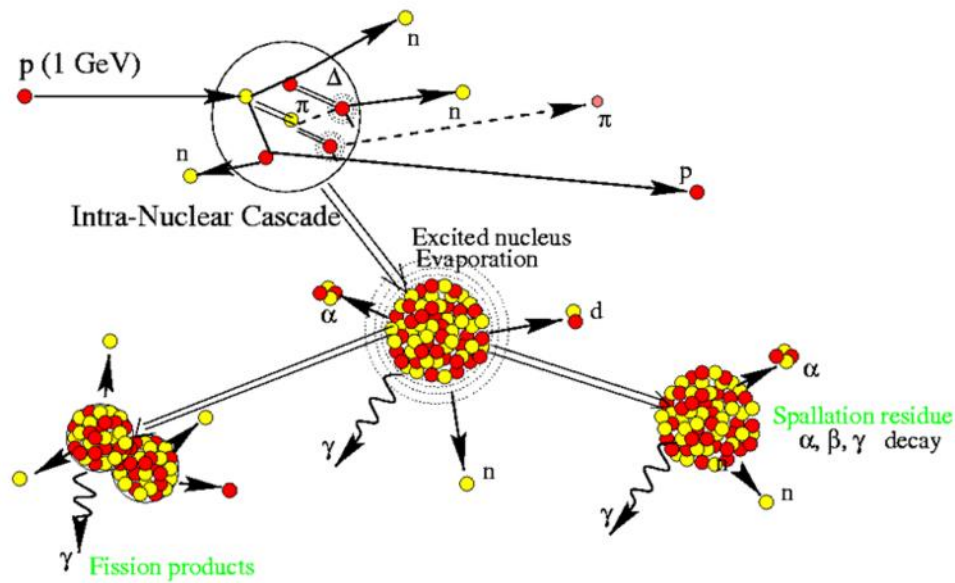


Figure 3.1. Spallation reaction (<https://www.google.com.tr>)

3.1.2. Spallation Target

In the spallation nuclear reaction, Bismuth + Lead (Bi + Pb) is used as the liquid metal of the mixture (Bi + Pb) or generally liquid Pb as the target material. A spallation is a form of reaction that is applied to produce more neutrons than to fission. Figure 3.1 shows schematic of spallation reaction. The spallation Pb target in the reactor is typically 60 cm in length and 20-50 cm in diameter. In the Accelerator Driven System (ADS), the Pb target interacts with the proton beam (Intra-nuclear Cascade). Interaction with target nuclides near high energetic nucleons generated during the "spalling" process when the proton beam is stopped in such a thick target is in the form of the inhibition (Karadeniz et al. 2001).

3.2. Accelerator Driven System (ADS)

Accelerators are devices that allow charged particle bundles such as electrons (e^-), positrons (e^+), protons (p), and anti-protons (p^-) boundless to accelerate up to to energy transfer determined within a specified purpose. Accelerators are used to extract these charged particles from higher energies. Accelerators are needed when the required accelerated particle is not available in natural ways or in laboratories. By means of these accelerated particles, studies are mainly being made on Basic Particle Physics and Nuclear Physics (yavas 2004).

3.2.1. History Of Accelerators

Despite the fact that the first particle accelerators were set up in 1930, important discoveries about the basic particles until 1950 were obtained in the cosmic ray experiments (for example, the presence of entities and strange particles). The main reason for this was that the energy available at the accelerators was low. The upgrading of these energies has been brought about ten times per decade with the help of advanced technology, and especially as a result of the establishment of the multipliers, the accelerators have become the most important devices for examining the structure of the material, their properties and their interactions (Sultansoy 2001).

3.2.2. Developments Of Accelerators

After the right and new atomic model revealed by the Rutherford experiment at the beginning of the 20th century, the human being has been accelerated in the search and effort of analyzing the basic structure of matter, especially in the high energy physics (particle physics) and accelerated new experiments in nuclear physics to use it. Cathode rays can be referred to as the first accelerators that generate electron currents between the tube cathodes and anodes.

In late 1920, Widereo had designed and launched the first modern linear electron accelerator (Linac). Cockcroft-Walton electrostatic accelerator was also realized in the same period. In 1932, protons accelerated by the Cockcroft-Walton proton accelerator were sent over Li nuclei, revealing two he nuclei. Higher electrostatic acceleration potentials were obtained with the Van de Graff generator. With this accelerator, MeV was reached as energy. (1 eV: the energy that an electron will gain by passing the potential difference of 1 Volt: 1 MeV = 10^6 eV) it is also the case that reaching a few MeV energies with induction linear accelerators is the same. The use of such accelerators with 30 drifting tubes after accelerating particle acceleration of resonant cavities (resonance cavities) stimulated by RF oscillation (~ MHz), as proposed by Widereo, accelerated the galvanic ions to an energy of 1,26 MeV (TAEK 2007).

3.3. Accelerators

Accelerators used in nuclear physics and particle physics research are generally divided into two groups;

- 1-Users who use DC voltage difference during acceleration
- 2-Users of radio frequency oscillating electromagnetic fields

At the beginning of the high-voltage accelerators are Cockcroft-Walton and Marx. By developing such accelerators, Tandem Van de Graff accelerators, which are widely used today, have been developed.

3.3.1. Tandem Van De Graff Electrostatic Accelerators

In this type of accelerators, ~ 25 MeV terminal voltages is produced by means of a smooth conductive surface or by means of an ion source and transported to a high voltage terminal by means of a moving beam. In such accelerators, negative ions are first accelerated from the ground lead to the high positive voltage terminal and the effective voltage reaches the mega-volt range. This voltage travels through a metal in the reaching beam vacuum system to extract electrons and positive ions are accelerated back to the ground potential. In this way, the accelerator produces high energy, but it is not as dense as the energy.

In such accelerators, where efficiency is low, the electrostatic bundle current is 10-20 μA . It is a disadvantage that such accelerators have a certain range of operation. Another disadvantage is that the negative ion source is initially used and is less when compared to positive ion sources. But despite all of this, it is widely used (Ertürk and Boztosun 2004).

3.3.2. Linear Accelerators (Lin Ac)

There is no need to re-accelerate ions using small potential differences in linear accelerators using radio frequency. In linear accelerators, ions are injected into a linear tube with a number of electrodes placed on it. The alternating voltage applied to both sides of the electrodes is suitably modified by changing the phases of the electrodes arranged at certain intervals to accelerate the ions moving. In 1928, a linear accelerator designed by (R). Wideroe accelerated positive ions of 50 keV and was used to accelerate both electrons and

protons after the second world. The 3 km long linear accelerator found at Stanford University is the longest linear accelerator, accelerating 50 GeV electrons or positrons (Ertürk and Boztosun 2004).

3.4. Total Reactions Cross Sections

CEM03.01 code calculates the sum of the door responded occasional act of Monte Carlo method using cross-sectional geometry. Our analysis has shown many different reactions in the incident, which occurred in different energies below about 100 MeV this systematics generally cross-section is inelastic best describes the Monte Carlo method, and it is not worse than Monte Carlo method in the higher energies. Therefore, we chose this systematics as the default for the normalization of all the results CEM03.01 code printed cross section. The overall response is calculated in the output of systematics CEM03.01 code described as inelastic cross section used here. (Of course, the user may normalize all the results CEM03.01 code to Monte Carlo overall reaction across departments by making a small change to the code in the routine type out), (Cossov 2002).

3.5. Production Of Residual Nuclides

Reliable cross-sections for the production of the remaining radionuclides from medium power and proton-Reactions caused by neutron ADS's necessary to calculate the radioactive inventory of the spallation target, of construction materials and the surrounding material. Production of the remaining radionuclides by GeV protons in thick or large targets are displayed complex modeling that you need to follow in detail chains between states and within the nuclear, production of primary, secondary and transport particles. Spectra of primary and secondary particles strongly depend on the radioactive material as well as on the geometry and depth into the goal.

To calculate the activation and radioactive rates and be folded stocks these spectra calculated with cross-sections that rely on energy from latent nuclear reactions energies of thresholds up to the initial energy of the primary stage particles. At present, there is no model or code available the required cross sections to predict with accuracy better than a factor of two on average. Therefore, one has to rely important nuclides on the experimental cross sections. There is a need for such experiments cross sections also if one tries to improve the forms and symbols as a basis for validation.

Given the importance of nuclear reactions of secondary particles, neutron-induced reactions that will control the inventory of radionuclides to the target fragmentation even though the primary high-energy protons it will contribute significantly. As a result, one needs cross-sections for both proton- and neutron induced reactions to models that can be relied upon to produce annual remaining on the entire energy group. Data that will be identified in this section will provide an experimental basis for calculating such spallation target stocks, shielding and construction materials to speed driven a few minutes after the system shut down, as well as to verify the theoretical work which is necessary for the health of radionuclides short-term account too are an essential part of the spallation target during the operation of the facility. With respect to the behavior in the long term and final disposal of spallation targets and construction materials and modeling the exact long Lived radionuclides have necessary. So far, there are no inventory calculations which take into account the long-lived radionuclides, mainly due to the absence of all cross-sections. For modeling radionuclide inventories will be sufficient as a first approximation has up to 200 MeV neutron cross sections. Measurements of the remaining annual production resulting from the neutrons are expected between 30 and 180 MeV. Reactions caused by proton and one that needs full functions excitement up to the energy of the primary beam (Gloris et al. 2001).

3.6. Light Charged-Particle Production

In here allocated to this part of the collection of data related to the recovery charged particles light. These data important for the investigation of high-energy nuclear competition models between neutrons and charged particles, and the emission of the nucleus of the vehicle (Deuterons, Alpha rays) are it has not yet dealt with in a satisfactory manner. Moreover, the proceeds of the production of hydrogen and helium are necessary for estimated gas production in the framework or structure of the material from the ADS. Sections are measured across the production of hydrogen and helium, using silicon 4π ball detector. So far, experiments have been conducted on the 0.8, 1.2, 1.8 and 2.5 GeV on several targets, and it expects further experiments. It is also performed these measurements in conjunction with the dividend neutron multiplicity. This allows the study of the rates of production of protons and alpha rays as the function of the excitation energy in the remaining core in intra-end of the nuclear cascade the stage. Will all this data and compared to high-energy nuclear models analysis. The implications of the results of this trial for the production of gas in some of the components and it will be evaluated for ADS, for example

on the age of the window or on the material structure. Moreover, a new magnetic spectrometer capable of measuring with high precision double differential cross sections for the production of light charged particles (caused by protons) in it will be a coincidence design with low-energy neutrons (Letourneau et al. 2000).

3.7. Production Of Residual Nuclei In Reverse Kinematics

In spallation reactions of heavy nuclei caused by protons of about 1 GeV, mostly short-lived radioactive nuclei are produced. It is shut down remains of fragmentation into the goal. Wear out towards stable isobar mostly through beta decay. After irradiation, long-lived radioactive waste time to be determined by mass spectroscopy and atomic number by gamma rays and mass accelerator spectrum. The availability of these tests reliable and comprehensive data on the revenue accumulated from and activities that can be inferred lived a long time and the proceeds of the final element. In addition, these techniques allowing more than a wide range of energies for the bombing of measurements. And compared with the previous the data revealed that the account available with a nuclear reaction models are not realistic enough but it is to pin down the shortcomings of the models on the basis of cumulative returns. For this the purpose, the whole methodology of isotope production cross-sections out of the nuclear there is an urgent need for a reaction. This means that these experiments provide unique and valuable information that complements the results that have been obtained in natural science movement. Because of the electronic interactions in the target fragmentation, initial proton loose energy and stimulate energy nuclear reactions in a wide range. However, the higher energies are of particular importance for the remaining products. The nucleolus, since more than 75% of the principal of the protons 1 GeV nuclear reactions in the spallation source in the energy group subject above 700 MeV. The aim of additional measurements with liquid deuterium target to provide information on spallation reactions caused by the neutron. Accounts activities, radio-toxicities distributions element of fragmentation leading Unreal It will be targeted using the means of transport and the development of codes implemented. Cross sections of elementary born from old nuclear models will be replaced either by the latest version of models J. Cugnon, or directly from the proceeds of the production is measured in the lead in 0001 electron volts (Wlazlo et al. 2000).

3.8. Codes And High-Energy Models

High energy codes, though universally successful to some extent, suffer from some deficiencies. Both from the comparison between the current and comparison with experimental data reveal, in some identified system contradictions that exceed the precision required by engineers who are working on projects ADS or spallation sources. These observations call for improvements to the physics already listed in a series of symbols (corrections, on average, the Pauli principle, which means the dynamics of the field), for evaporation codes (intensity level) and fission codes (viscosity, evaporation fission competition in high-energy excitement). These improvements are part of a task specific theory in this project. The first step will consist of improving the existing codes by including aspects of physics not included so far, through the modification of some physics that is already implemented. Improving Pauli blocking, this represents a lot of fluctuations, and improvements in the medium corrections. To me evaporation symbols, the first step involves careful examination of the data entry and advanced the development of fission model in the high-energy excitement, and take advantage of imminent fission component in the science of measuring the reverse advances in nuclear dynamics far from equilibrium. The aim of the second step in the ratification of the improved laws (and other standard symbols), the data for each of the thin and thick target. In addition, compare and wide however experimental production residue to be provided by realized data. And a third step, it will make new improved icons, if necessary.

This work will involve modifying the parameters presented to describe aspects of physics is less well known, such as the parameters regulating coupling between the intra nuclear cascade and evaporation symbols and some parameters fission model, especially viscosity. The ultimate goal will consist of a copy of the code of high energy transfer (Cugnon et al. 1997).

3.9. Method

Cross-section of the interaction of particles creates accelerated nuclear physics, in particular, the task in the field of medical science. This type of reaction that may occur during the creation of cross-sections of the problems in order to eliminate or publishing spectrum experimental measurements and theoretical calculations must be performed in order to determine the circumstances that may occur in early. For example, the maximum chip that can send energy range of particles before, or sent to the energy range of particles to see which should show the importance of this account. On the other hand, for the excesses of the main problems with different models of nuclear physics to calculate the theoretical role of nuclear interaction and control of a pilot is required. Study the effect in more detail in different sections of the energies of nuclear reactions and spectral shape for delivery is important.

3.10. The Nuclear Model

It is obtained on the active neutrons required before the end of nuclear testing. It is possible to say that the energy spectra of neutrons and the formation of particles obtained by the move after these experiences. However, considering the consistency of models of the spectrum of the cross-section of the effect of the particles of the molecules to be formed with the theoretical calculations before and after the experiment, we will avoid all of the loss of time and masculine unnecessary. It can also be calculated values of this theory department and the spectrum through the use of some forms of the nuclear package. However, the discussion of the accuracy of these values calculated after comparing and interpreting get pre-testing and data acquisition as a result of these experiments, and after calculating the error share they have. The fact that particles with energies high-order, which has not been tested with more of these models, are able to cross section and calculate the spectra of the particles through the new isotopes that will form after the bombing, which makes use of attractive models. We found a solution to the disorder (interaction) theory of time-dependent quantum mechanics in the first order for the fifth and then is passed to the density of the state.

$$H=H_0+V \quad (3.1)$$

Here; H_0 belongs to the stable elements. We found a solution to the disorder (interaction) theory of time-dependent quantum mechanics in the first-class V-Density. Solve this system constitutes the lower part of the pre-equilibrium models (Yıldırım 2009).

3.10.1. Pre-Equilibrium Reactions

Nuclear reactions can be studied under two categories. First, the immediate reaction and it creates a very quick process. This type of reaction time occurs about 10^{-22} seconds. This accelerated period of particles called to pass through without any interference from the target nucleus. The second type of interaction; nuclear reactions vehicles, and the reaction time is 10^{-16} seconds on average, which is far from a direct response did longer. When studying nuclear reactions with statistical methods is the microscopic examination of vehicles in the sense of direct and reactions.

For work, about the reaction of neutrons created by nuclear reactions in the first year of the vehicles and head of studies that directly interact, it was noted the existence of a mechanism before the balance (Holub et al. 1980). Balance mechanism next, depending on the nucleus of the target and vehicle systems in mass exciton initial energy neutrons, protons, and the play is more important than other types of reactions to the launch of an alpha particle role (Milazzo of-Cole and Braga- Marcazz 1974). The experiments indicate the presence of President of the Third reactions of nuclear reactions and compounds directly. This is called pre-reaction equilibrium. In such particles react with compounds form the two chambers nuclear by collision system is deployed in the period between fully reach the thermal equilibrium of the system or statistics. This is especially important in high-energy part of the spectrum published molecules.

The main models that examine pre-equilibrium reactions are:

- 1- Full Exciton Model.
- 2- Hybrid Model
- 3- Geometry Dependent Hybrid Model
- 4- Cascade-Excited Model

3.10.2. Common Characteristics Of Pre-Equilibrium Models

In this study, we mainly 4 models used. Of these, only model cascade exciton of high-energy group (GeV) for making the calculations, while the other three models, medium-energy balance is able to react before the calculations. These models are similar in some features. All models include statistical methods. It uses a jamming of Hamilton's theory of mathematical calculations used to the maximum level of all the calculations. It is another common feature, in practice with the aid of this model is that it can calculate the running total spectrum of energy particles and occasional sections. Prior to this experiment, it will facilitate the work of researchers and give them an idea of the experience. Also, with the use of statistical methods in each of these models, and the structure of the impact of the core angular momentum in the calculations taken into account (Kalbach 1975).

3.10.3. Full Exciton Model

This model, because of the goal after the first interaction between the particles at the heart of the system will be notified of the result exciton energy entering the system, and says that there will be complications in the system. However, it is supposed to be accessible to the complexity of balance again after passing through a series of steps. This shows that these steps occur by way of the spread of terrestrial energy are required to enable the system each. This is because the energy emitted particles can be touched and stimulated excited different molecules and processing complexity, classified according to their number. In this model. The basic probability of particle by the state and one put it there on equal terms. You sent when the particles in the target solid 1P-0h (or 1-exciton) case, with one of the nuclei of the core objectives of interacting 2P-1h (or 3 excitons) is created the center. Here p; the number of particles is h. It refers to a reference number. Interaction creates a later supplemented with state-mentioned particles composed more than doubled. Also exciton model "is in balance operations. It is possible to calculate the probability of the particles released during this process. In this calculation method, as well as creating a direct numerical solution of the equation, Mr. Pauli. The main advantage of this model a nuclear reaction is a function of time. This information is defined in equation 3.3.

$$dP/dt = \lambda^+ (n-2) \tag{3.2}$$

$$P(n-2,t) + \lambda^- (n+2) P(n+2,t) - \{ \lambda^+(n) + \lambda^-(n) W(n) \} P(n,t) \tag{3.3}$$

In equation 3.3, $P(n,t)$ is the probability of being in the exciton state. The transient velocities of $\lambda +$, $\lambda - n \rightarrow n + 2$ and $n \rightarrow n - 2$ are the velocities of the particles in all energies from the exciton state of $W(n)$. Here, the initial condition for the main equation system is; The number of starting particles $p_0 = 2$ and the number of starting hypotheses $h_0 = 1$ for the reactions formed with nuclei $P(p,h,0) = \delta(p,p_0) \delta(h,h_0)$. The integral of the cross section is calculated by $d\sigma / d\varepsilon = \sigma_a \Sigma W b(n,\varepsilon) \tau(n)$. Where σ_a is the reaction duration, $\tau(n)$ is the average life in the case of n excitons and $\tau(n) = \int_0^\infty P(n,t) dt$ it is the average life from the integration of $t=0$ to $t=\infty$. $Wb(n,\varepsilon)$, b is the fraction n . Average speed from exciton step (Kaplan et al. 2009).

3.10.4. Hybrid Model

Hybrid Model; Exciton Model "as it is landed, it accepts single particle states as equidistant placement. It classifies the core states as well as the excited particles and debris. The nucleon, as it was said before, forms the state $1p - 0h$ of the target nucleus. Then it interacts with the target nucleon to generate $2p - 1h$. Thus, the two-body interactions cause more particle-tooth pairs to form. This model calculates the distribution of the exciton energies of the excited particles for each nuclear state. For each particle exciton energy, partial particle emission rates are calculated based on the new particle-droplet formation. While this calculation is initially initiated with a $2p - 1h$ configuration, all cases are considered in turn. In particle publishing, all processes contribute to the pre-equilibrium spectrum. This process continues until the number reached a better balance in the system exciton possible. Then, there are more than standard vehicles account for the remaining period of response did the basic model. Thus, the target nucleus and send by particle interactions of particles until it doubles this model, which led to the formation, we can talk without pre-compounds degradation.

This decomposition also,

$$P_v(\varepsilon) = \sum_{\substack{n=n_0 \\ \Delta n=+2}}^n [n \chi_v N_n(\varepsilon, U) / N_n(E)] g d\varepsilon \{ \lambda_c(\varepsilon) / \lambda_c(\varepsilon) + \lambda + (\varepsilon) \} D_n \quad (3.4)$$

$$d\sigma(\varepsilon) / d\varepsilon = \sigma_R P_v(\varepsilon) \quad (3.5)$$

$P_v(\varepsilon) d\varepsilon$; The number of particles of type v (neutron and proton) between the energies ε and $\varepsilon + d\varepsilon$ and continuing to the region, n ; The most probable number of excitons at equilibrium

position, n^z_v ; The number of particles in type v in an exciton state, E ; Exciton energy of the compound system, $N(\varepsilon, U)$; $I_n(E)$, where n is the number of arrangements of excitons in an appropriate manner, as will be shared among the other $n-1$ excitons of exciton energy $= E - Bv - \varepsilon$ when emitted by an exciton ε channel $N_n(E)$; particle plus gradient in exciton energy n ($n = p+h$) total number of junctions, $\lambda_c(\varepsilon)$, in the exciton energies; The velocity of a particle (ε) to the continuous zone through channel energy, $\lambda + (\varepsilon)\varepsilon$; D_n is the in-core velocity at which an energetic particle is continuously propagated to the region; The initial population section in an n -exciton chain, σ_R ; Reaction effect section, g ; Refers to the single-particle level intensity. The quantity in the brackets in 3.4 above gives the number of particles between the continuous zone energy ε and $\varepsilon + d\varepsilon$. The expression in the second parentheses is the ratio of the continuous velocity to the continuous velocity of the continuous zone (Aydin et al. 2007).

3.10.5. Geometry Dependent Hybrid Model

Balance is a pre-engineering model dependent hybrid model is a copy of the equation with the definition of nuclear exciton employed formation within the nucleus scattering nucleus. This model mathematical calculations by (Blann and Vonach 1983),

$$d\sigma_v(\varepsilon)/d\varepsilon = \sigma_R P_v(\varepsilon) \quad (3.6)$$

And

$$P_v(\varepsilon)d\varepsilon = \sum_{\substack{n=n_0 \\ \Delta n=+2}}^n [n\chi_v N_n(\varepsilon, U)/N_n(E)] g d\varepsilon \{ \lambda_c(\varepsilon)/\lambda_c(\varepsilon) + \lambda + (\varepsilon) \} D_n \quad (3.7)$$

As used in Eqs. 3.6 and 3.7, σ_R ; Reaction cross section, n^z_v ; N is the number of v type particles (proton or neutron) in the exciton state, $P_v(\varepsilon)d\varepsilon$; Shows the number of v typed particles (protons or neutrons) that are continuously transmitted between the energies ε and $\varepsilon + d\varepsilon$. Also; $\lambda + (\varepsilon)$ is the rate at which a particle (ε) propagates to the continuous region with channel energy, $\lambda + (\varepsilon)$; ε is the in-core velocity of an energetic particle, D_n ; The initial population section in an n -exciton chain, σ_R ; Reaction effect section, g ; One-particle level intensity. Thus, the quantity in square brackets in Eq. (3.7) gives the number of particles between energy ε and $\varepsilon + d\varepsilon$; In the second parentheses, the transit velocity of the particles to the reaction zone, To the total particle velocity (Kaplan et al. 2009). Also in this model, the extreme particle-to-state density from the cross-section is important, and particle

nucleation formation is dependent on the nuclear surface. That is why there is a small difference in the energies in the constant region. In addition, it is observed that the Hybrid Model is separated due to the angular contribution of the absorbed particle and the angular variation of the extraneous particle to be released.

3.10.6. Cascade Exciton Model

Cascade exciton model (CEM) is another calculation method used to calculate the pre-equilibrium calculations of the reactions between the non-energetic particle and the target nucleus. Carry out exciton processing of the target particle of the particle sent to the target. Then, this emerging nuclear system begins to emit particles until it reaches a statistical balance. This publishing mechanism; Are examined according to the distortions of the formed composite core and the direct interactions. Use of equilibrium and pre-equilibrium models; to understand the nuclear structure and to explain the mechanism of particle ejection. Many features of nuclear reactions in high energies can be examined in a very good way, taking into consideration the transient post-processing (Cascade) in nuclear levels. The Cascade Model assumes that reactions occur in three stages. First stamina, nuclear transitions in levels. The second phase corresponds to the equilibrium (or compound core) state before the equilibrium and the third phase corresponds to the equilibrium (or compound core) state. In general, these three stays contribute to the experimentally measured values. Accordingly, for the particle spectrum;

$$\sigma(p)dp = \sigma_{in} \{N_{cas}(p) + N_{prq}(p) + N_{eq}(p)\} dp \quad (3.8)$$

In this equation, and inelastic scattering cross-sections, calculated in a row in the transformation model. However, they are independent of the accounting visual model; so many times in this model, the normalization of the expense and there is a need for additional data.

The cascade model accounts for the reaction geometry that holds all the information about the kinematic characteristics of fast particles. However, the interactions between these particles are neglected. On the other hand; excited model is an excited nucleus; hh, Ph, and PP (ie, "particle-dynamic" degrees of freedom are included) are considered as half-particle gasses that account for the interactions cascade model phases are realized when the kinetic energy of the incoming particle exceeds the coupling energy of the nucleus. It is important

to combine these two models in order to develop the definition of the nuclear reaction properties of the particles emitted in a large energy region. Also, for cascade exciton model; accelerated particles and core are considered as two different species, and fluctuations are seen among the energies given in the calculations since distortions between these particles are neglected (Sarier et al. 2009).

3.11. Evaporation Model

Evaporation model description carries balance nucleus with excitation energy balance has been reached at the end of the pre-equilibrium phase. The possibility of the decay of a nucleus to a specific channel depends on the intensity level in the channel and the possibility of traffic through the energy barrier occurs. As a result of a competitive process for the balance of decay, it can happen at high energy (Dreiser 1962).

4. RESULT AND DISCUSSION

4.1. Calculation Method

In this study, the reaction cross section and run isotope of heavy elements are calculated using equilibrium and pre-equilibrium nuclear reaction models. In calculations; to examine pre-balance effects; cascade exciton, hybrid and geometry additive hybrid model was used. ALICE / ASH computer program codes are used for cascade exciton model, CEM03 (Mashnik 1980) and hybrid and geometry additive hybrid calculations.

Isotopes of different elements ^{82}Pb , ^{81}Ti , ^{84}Po , ^{73}Ta , ^{75}Re , ^{72}Hf have been obtained at $p + ^{74}\text{W}^{184}$ and $p + ^{83}\text{Bi}^{209}$ reaction with protons having different energies. Reaction cross sections isotope productions have been calculated. Calculations have been made with CEM03 and ALICE/ASH code.

4.2. CEM03 Computer Program

The cascade exciton model CEM03 accounts (Mashnik 1980) using a computer program. Reactions nucleon-nucleus in the field of medium power appropriate to examine the balance before the deployment of the particles. In this atomic number (Z) of the program, the number of neutrons (N) is the total energy of the particles (E). The CEM03 program design Cascade-exciton to Monte Carlo calculations of nuclear reactions in the framework of the model. CEM03 program, flexible reaction, fission and the total cross-section, the functions of the excitement and energy distribution of the nucleus and angular spectrum, the double differential cross section, and multiply on average, and the average energy of the production sectors through products managed an account. CEM03 listed "various models to calculate the e parameter intensity level. This program uses the cascade model calculations exciton. Cascade-exciton model (CEM) reaction to the three stages of thinking (Demirkol, 2003). The first stage is the nucleus cascade.

At this stage, it can be elementary particles scatter several times before absorption or escape from the nucleus. The second phase of the starting point for the pre remaining balance after the issuance of the particle chain alerted particles incurred from waste nuclear reactions. Equilibrium third phase (evaporation) is the stage. Is nuclear warning treatment prior to the deterioration of the balance settlement exciton model (Demirkol 2003).

The cascade model adds responded engineering reaction that contains all the information about the kinetic properties of the particles fast account. However, it ignores the interactions between these particles. To improve the definition of response nuclear reaction of emitted particles properties over a wide energy region is important that the combination of these two models. In addition, cascade exciton model; considered particles and nuclei accelerated two different collisions between these particles due to neglect. CEM of nuclear reactions was proposed 25 years ago at the laboratory of theoretical physics; the joint institute for nuclear research. It was extended to consider photonuclear reactions (Gabriel et al. 1994).

4.3. ALICE / ASH Computer Program

ALICE / ASH (Broeders et al. 2006) (Blank, 1991) program is a slightly modified version and strengthened. ALICE / ASH has maximum 300 electron volts, "such as coming to power. Function exciton, the product consists of a spectrum of energy distribution angular secondary particle, and the accounts of the accidental and scalable section of the application of gentle delivery (Demirkol 2003).

This computer code can perform various types of calculations and combinations of these types:

1. A standard Weisskopf-Ewing evaporation calculator with multiple particle emissions (Weisskopf 1940). Emitted particles may be either neutrons; n and p; n, p, and α ; or n, p, α , and d. Excitation energies of up to 200 MeV of the compound core can be considered. A grid of 9 mass units in depth and 11 mass units in width by 9 atomic numbers deep may be calculated from the residual nuclei (evaporation residue yields) code is now dimensioned. The particle spectrum can be selected on the output in addition to the individual product yields and the fission cross-sections.

The reverse reaction sections can be read out from the cards, calculated using a classical sharp cut off model, or calculated by an optical model subroutine by default. (The second option was to calculate the evaporation steps with 1 MeV bin widths (Blann 1966), resulting in approximately 95% of the total calculation time used.

2. In this option, wave approach (Ericson 1960), (Blanks 1965), which gives an upper limit to the increase of the γ radiation, can be chosen, calculation (1) is carried out for each partial wave in the input channel and is irreversibly connected to the cyclic motion of the rotation energy for each partial wave and therefore can not be used for particle emission. The rotational energy versus J may be selected either as the rigid spherical rotor value, or from the equilibrium deformed rotating liquid drop model of (Cohen et al. 1974) the transmission coefficients for the entrance channel partial waves to be used in the computation may be read in from cards or by default will be provided by the parabolic model (Thomas 1959) routine (projectile atomic number ≥ 2) or by the optical model routine (n, p, d).

3. Evaporation calculations may involve fission competition using angular momentum dependent ground conditions and saddle-point energies (Bohr 1939). The latter values come from the (Cohen et al. 1974) rotating liquid drop calculations. Calculations are made for each partial wave; the upper and lower limited on the angular momentum can be selected (in other words, the calculation may be limited to an angular momentum 'window'). In addition to some multiplier factors, provision has been made in the introduction to change the ratio of saddle point level densities (a_f/a_n) to the base state (default = 1). It is assumed that the nuclear momentum of the nucleon emission, daughter core, is reduced by 1 K from the parent nucleus. This is a very arbitrary approach, and it is better to use more rigorous codes when detail in angular momentum removal is important. The option exists to read fission barriers in for each nuclide rather than using RLD results. This is important as Z increases and the liquid drop contribution to the fission barriers is less than Strutinsky / shell effects. Provision is made to allow pre-compound emissions via hybrid models based on hybrid/geometry. When this option was chosen together with fission the authors have assumed that the fast pre-compound process will precede fission with no competition. As excitation energies increase and fission and evaporation widths increase, this assumption may become invalid. However, also be noted that the basic criteria of the compound nucleus model are not met and that the fission and evaporation theoretical validity that the calculations are suspicious.

4.4. $p + {}_{83}\text{Bi}^{209}$ Reaction

Bismuth (Bi) is a chemical element in the periodic table symbolized by the symbol Bi, which has an atomic number of 83. It is called German Weisse Masse, meaning white mass. Bismuth belongs to the weak metals. For a long time, he was confused with lead or tin until 1753, when Claude Geoffroy Le Joun could separate him from bullets.

Is the "almost stable" counterpart of bismuth with the longest half-life known to any radioisotopes that undergo α -decay (alpha decay). It has 83 protons and magic (physics) of 126 neutrons, and an atomic mass of 208.8803987 amu (atomic mass units).

Properties: A heavy chemical element, its mass of 209, its symbol Bi and atomic number 83 belongs to a group of nitrogen, light pink, light and heavy, it is the second worst conductor of heat after mercury, its electrical resistance is relatively large for a metal, and it increases with the magnetic field, a magnesia metal, know that it is less heavy metal toxicity, it has a lower density in its liquid state than its solid state.

Uses electrophoresis: In the form of an alloy with bismuth and tin, this has a low melting point, such as fire protection, in glassware and ceramics.

4.4.1. ${}_{83}\text{Bi}^{204-209}$ the product ion resulting from the reaction of $p + {}_{83}\text{Bi}^{209}$

The formation cross section of the ${}_{83}\text{Bi}$ isotope with the different mass number (A) have been obtained for reaction $p + {}_{83}\text{Bi}^{209}$ at energy $E_p = 50$ MeV. The product resulting from the reaction of the proton at different energies has been shown in Figure 4.1. The maximum formation level of isotope Bi^{207} is 226.9 mb and the minimum formation level of isotope Bi^{204} is 2.937 mb. The radioactive of Bi^{208} is 0.368 M year of Bi^{207} is 32 year and of Bi^{206} is 6.24 day.

Table 4.1. Mass number (A) cross sections obtained for isotope of ${}_{83}\text{Bi}$ at reaction $p+{}_{83}\text{Bi}^{209}$; $E_p=50$ MeV energy. Calculations have been made with CEM03 and ALICE/ASH and PCROS code

${}^{209}\text{Bi}(p,x){}_{83}\text{Bi}^{204-209}$; $E_p=50$ MeV				
Mass number (A)	Radioactive Half life	CEM03-Code Cross section (mb)	ALICE/ASH-Code Cross section (mb)	PCROS (mb)
209		56.98	49.3	722.557
208	0.368 M year (e)	163.9	133	
207	32 year (e)	226.9	223	
206	6.24 day (e)	186	185	
205		77.93	33.5	
204		2.937		

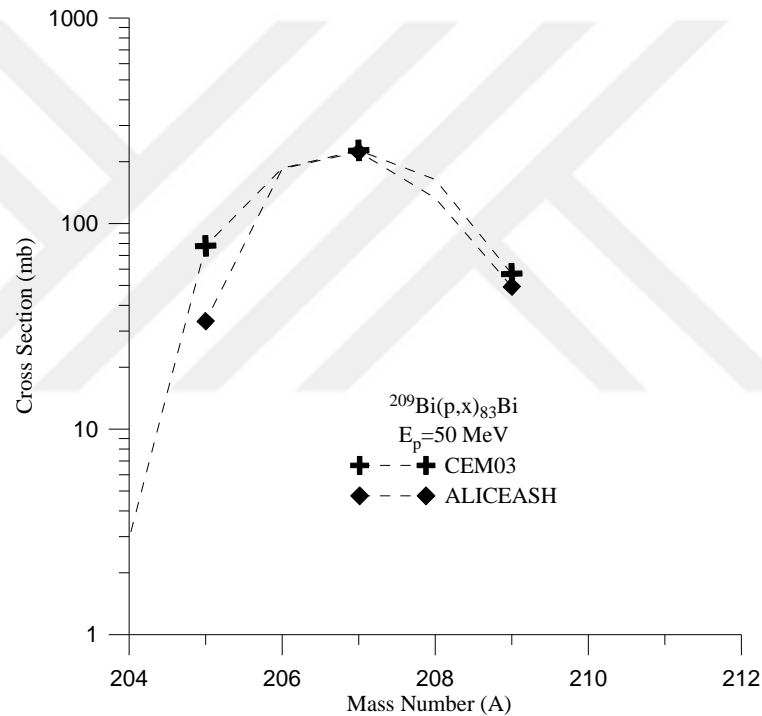


Figure 4.1. Mass number (A) cross sections obtained for isotope of ${}_{83}\text{Bi}$ at reaction $p+{}_{83}\text{Bi}^{209}$; $E_p=50$ MeV energy. Calculations have been made with CEM03 and ALICE/ASH code

4.4.2. ${}_{84}\text{Po}^{204-210}$ the product resulting from the reaction of $p+{}_{83}\text{Bi}^{209}$

The formation cross section of the ${}_{84}\text{Po}$ isotope with the different mass number (A) have been obtained for reaction $p+{}_{83}\text{Bi}^{209}$ at energy $E_p=50$ MeV. The product resulting from the reaction of the proton at different energies has been shown in Figure 4.2. The maximum formation level of isotope Po^{205} is 589.4 mb and the minimum formation level of isotope Po^{209} is 39.75 mb. The radioactive of Po^{210} is 102 year of Po^{209} is 2.90 year of Po^{208} is 138.4 day and of Po^{206} is 8.8 day.

Table 4.2. Mass number (A) cross sections obtained for isotope of ${}_{84}\text{Po}$ at reaction $p+{}_{83}\text{Bi}^{209}$; $E_p=50$ MeV energy. Calculations have been made with CEM03 and ALICE/ASH and PCROS code

${}^{209}\text{Bi}(p,x){}_{84}\text{Po}^{204-210}$; $E_p=50$ MeV				
Mass number (A)	Radioactive Half life	CEM03-Code Cross section (mb)	ALICE/ASH-Code Cross section (mb)	PCROS (mb)
210	138.4 day (α)			6.89821
209	102 year (α)	39.75	42.7	
208	2.90 year (α)	93.2	89.4	
207		117.9	131	
206	8.8 day (e)	280.4	291	
205		589.4	676	
204		39.75	102	

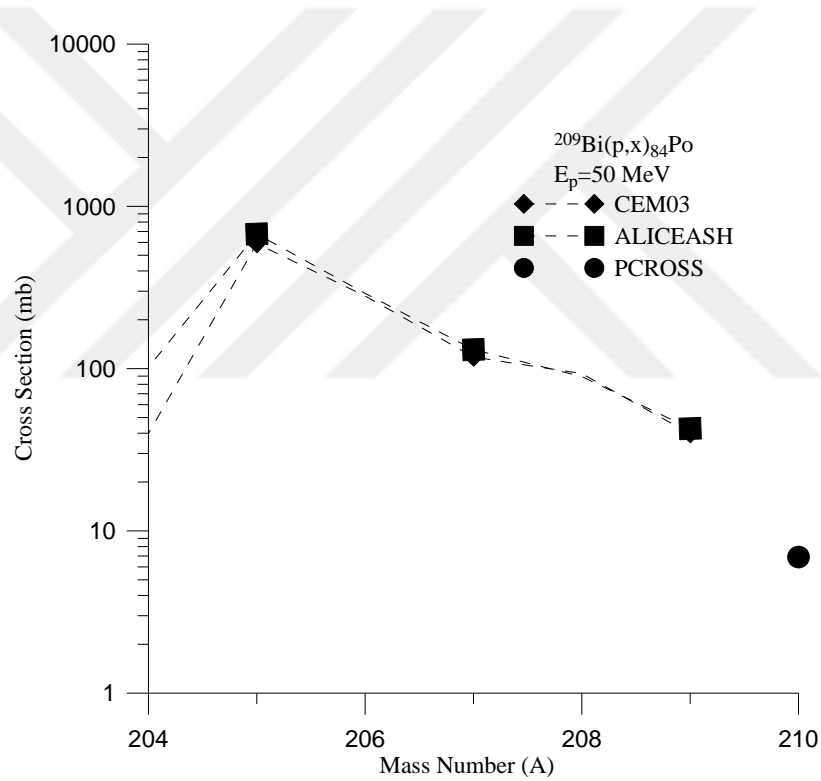


Figure 4.2. Mass number (A) cross sections obtained for isotope of ${}_{84}\text{Po}$ at reaction $p+{}_{83}\text{Bi}^{209}$; $E_p=50$ MeV energy. Calculations have been made with CEM03 and ALICE/ASH and PCROS code

4.4.3. ${}_{82}\text{Pb}^{198-208}$ the product resulting from the reaction of $p+{}_{83}\text{Bi}^{209}$

The formation cross section of the ${}_{82}\text{Pb}$ isotope with the different mass number (A) have been obtained for reaction $p+{}_{83}\text{Bi}^{209}$ at energy $E_p=100$ MeV. The product resulting from the reaction of the proton at different energies has been shown in Figure 4.3. The maximum

formation level of isotope Pb^{204} is 50.5 mb and the minimum formation level of isotope Pb^{199} is 2.82 mb. The radioactive of Pb^{205} is 15 M year and of Pb^{202} is 0.05 M year.

Table 4.3. Mass number (A) cross sections obtained for isotope of ${}_{82}\text{Pb}$ at reaction $p+ {}_{83}\text{Bi}^{209}$; $E_p=100$ MeV energy. Calculations have been made with CEM03 and ALICE/ASH code

${}_{83}\text{Bi}^{209} (p,x) {}_{82}\text{Pb}^{198-208}$; $E_p=100$ MeV			
Mass number (A)	Radioactive Half life	CEM03-Code Cross section (mb)	ALICE/ASH-Code Cross section (mb)
208		9.96	30.9
207		27.6	31
206		38.9	31.4
205	15 M year (e)	34.0	31
204		50.5	29.4
203		32.3	1.62
202	0.05 M year (e)	33.6	2.12
201		10.9	1.3
200		9.77	
199		2.82	
198		4.88	

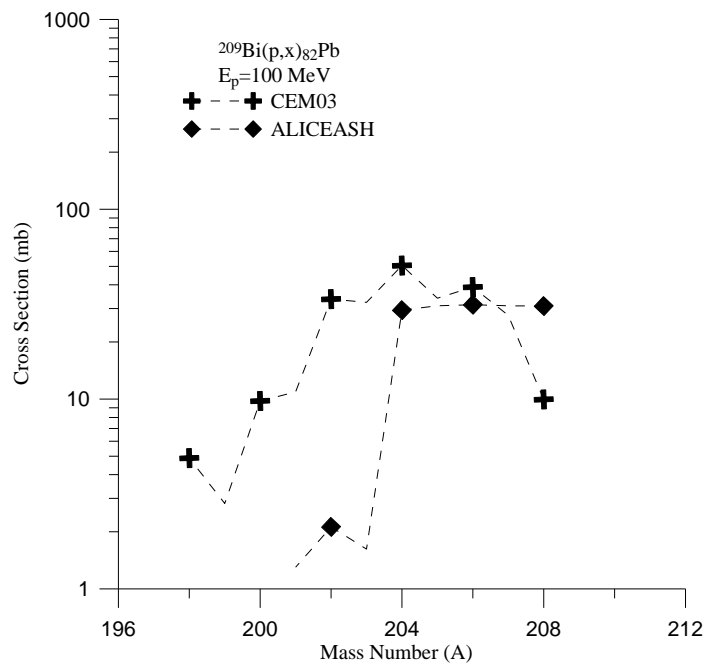


Figure 4.3. Mass number (A) cross sections obtained for isotope of ${}_{82}\text{Pb}$ at reaction $p+ {}_{83}\text{Bi}^{209}$; $E_p=100$ MeV energy. Calculations have been made with CEM03 and ALICE/ASH code

4.4.4. ${}_{82}\text{Pb}^{198-208}$ the product resulting from the reaction of $\text{p}+{}_{83}\text{Bi}^{209}$

The formation cross section of the ${}_{82}\text{Pb}$ isotope with the different mass number (A) have been obtained for reaction $\text{p}+{}_{83}\text{Bi}^{209}$ at energy $E_p=100$ MeV. The product resulting from the reaction of the proton at different energies has been shown in Figure 4.4. The maximum formation level of isotope Pb^{204} is 50.5 mb and the minimum formation level of isotope Pb^{199} is 2.82 mb. The radioactive of Pb^{205} is 15 M year and of Pb^{202} is 0.05 M year.

Table 4.4. Mass number (A) cross sections obtained for isotope of ${}_{82}\text{Pb}$ at reaction $\text{p}+{}_{83}\text{Bi}^{209}$; $E_p=100$ MeV energy. Calculations have been made with CEM03 and ALICE/ASH code and experimental data

${}^{209}\text{Bi}(\text{p},\text{x}){}_{82}\text{Pb}^{198-208}$; $E_p=100$ MeV				
Mass number (A)	Radioactive Half life	CEM03-Code Cross section (mb)	ALICE/ASH-Code Cross section (mb)	EXPERIMENTAL DATA (mb)
208		9.96	30.9	5.3
207		27.6	31	
206		38.9	31.4	
205	15 M year (e)	34	31	
204		50.5	29.4	
203		32.3	1.62	
202	0.05 M year (e)	33.6	2.12	
201		10.9	1.3	
200		9.77		
199		2.82		
198		4.88		

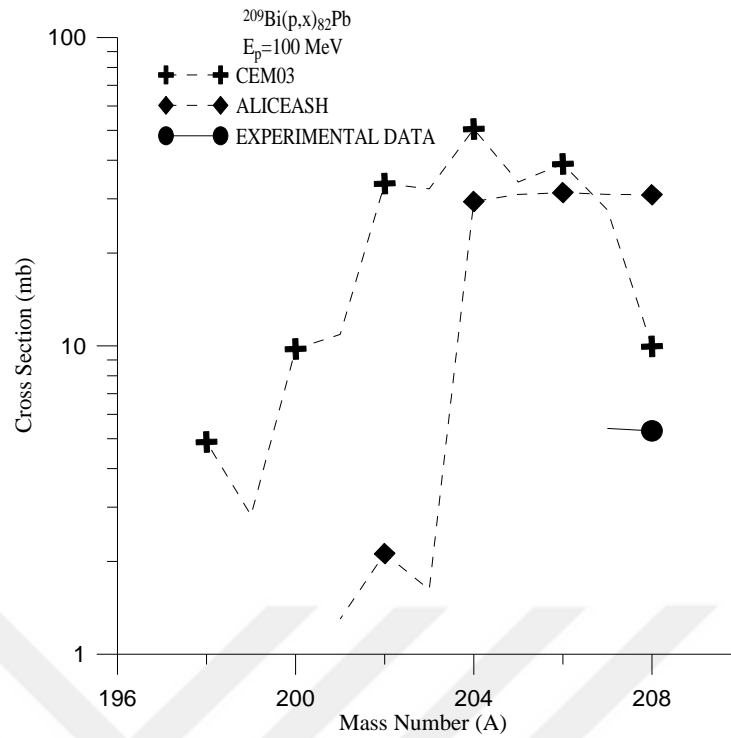


Figure 4.4. Mass number (A) cross sections obtained for isotope of ${}_{82}\text{Pb}$ at reaction $p + {}_{83}\text{Bi}^{209}$; $E_p=100$ MeV energy. Calculations have been made with CEM03 and ALICE/ASH code and experimental data

4.4.5. ${}_{81}\text{Tl}^{195-205}$ the product resulting from the reaction of $p + {}_{83}\text{Bi}^{209}$

The formation cross section of the ${}_{81}\text{Tl}$ isotope with the different mass number (A) have been obtained for reaction $p + {}_{83}\text{Bi}^{209}$ at energy $E_p=150$ MeV. The product resulting from the reaction of the proton at different energies has been shown in Figure 4.5. The maximum formation level of isotope Tl^{199} is 10.9 mb and the minimum formation level of isotope Tl^{205} is 1.41 mb. The radioactive of Tl^{204} is 3.77 year and of Tl^{202} is 12.2 day.

Table 4.5. Mass number (A) cross sections obtained for isotope of ${}_{81}\text{Tl}$ at reaction $p+{}_{83}\text{Bi}^{209}$; $E_p=150$ MeV energy. Calculations have been made with CEM03 and ALICE/ASH code

${}^{209}\text{Bi}(p,x)_{81}\text{Tl}^{195-205}$; $E_p=150$ MeV			
Mass number (A)	Radioactive Half life	CEM03-Code Cross section (mb)	ALICE/ASH-Code Cross section (mb)
205		1.41	
204	3.77 year (β^-)	4.04	
203		5.27	0.13
202	12.2 day (e)	7.74	
201		9.49	
200		9.49	
199		10.9	
198		6.68	
197		5.80	
196		3.52	
195		3.34	

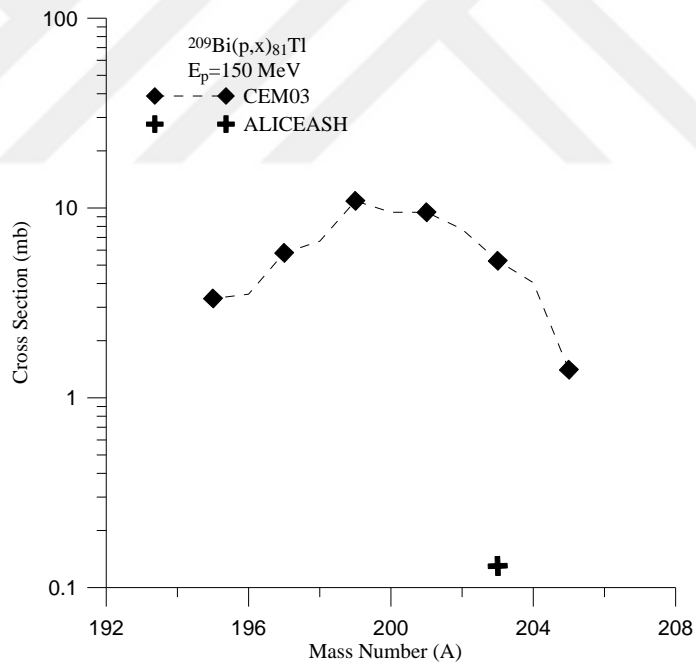


Figure 4.5. Mass number (A) cross sections obtained for isotope of ${}_{81}\text{Tl}$ at reaction $p+{}_{83}\text{Bi}^{209}$; $E_p=150$ MeV energy. Calculations have been made with CEM03 and ALICE/ASH code

4.4.6. ${}_{82}\text{Pb}^{194-208}$ the product resulting from the reaction of $p+{}_{83}\text{Bi}^{209}$

The formation cross section of the ${}_{82}\text{Pb}$ isotope with the different mass number (A) have been obtained for reaction $p+{}_{83}\text{Bi}^{209}$ at energy $E_p=150$ MeV. The product resulting from the reaction of the proton at different energies has been shown in Figure 4.6. The maximum

formation level of isotope Pb^{202} is 61.2 mb and the minimum formation level of isotope Pb^{194} is 1.58 mb. The radioactive of Pb^{205} is 15 M year and of Pb^{202} is 0.05 M year.

Table 4.6. Mass number (A) cross sections obtained for isotope of ${}_{82}Pb$ at reaction $p+{}_{83}Bi^{209}$; $E_p=150$ MeV energy. Calculations have been made with CEM03 and ALICE/ASH code

${}^{209}Bi(p,x){}_{82}Pb^{194-208}$; $E_p=150$ MeV			
Mass number (A)	Radioactive Half life	CEM03-Code Cross section (mb)	ALICE/ASH-Code Cross section (mb)
208		3.52	30.7
207		25.5	32.3
206		28.5	31.1
205	15 M year (e)	24.4	25.9
204		41.0	36.8
203		39.6	44.2
202	0.05 M year (e)	61.2	35.4
201		48.5	9.33
200		52.9	
199		36.4	
198		30.1	
197		13.7	
196		7.56	
195		36.9	
194		1.58	

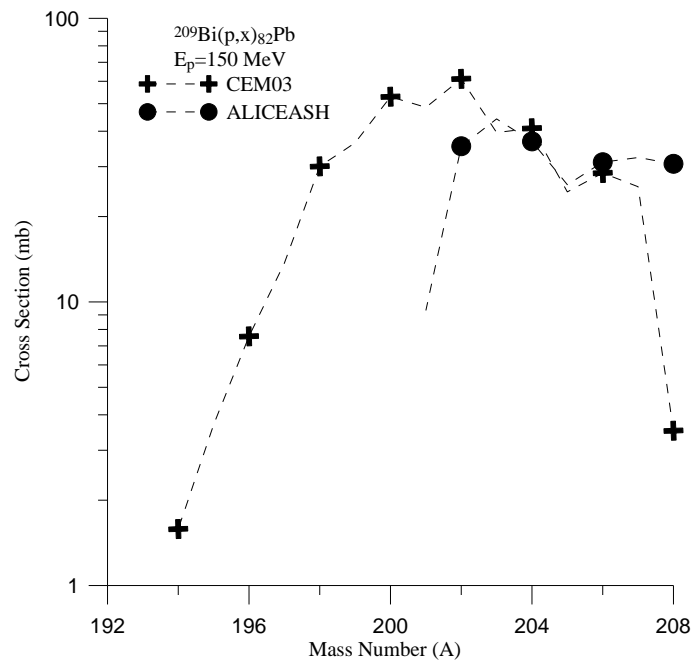


Figure 4.6. Mass number (A) cross sections obtained for isotope of ${}_{82}Pb$ at reaction $p+{}_{83}Bi^{209}$; $E_p=150$ MeV energy. Calculations have been made with CEM03 and ALICE/ASH code

4.4.7. ${}_{84}\text{Po}^{197-209}$ the product resulting from the reaction of $p+{}_{83}\text{Bi}^{209}$

The formation cross section of the ${}_{84}\text{Po}$ isotope with the different mass number (A) have been obtained for reaction $p+{}_{83}\text{Bi}^{209}$ at energy $E_p=150$ MeV. The product resulting from the reaction of the proton at different energies has shown in Figure 4.7. The maximum formation level of isotope Po^{202} is 48.2 mb and the minimum formation level of isotope Po^{197} is 4.92 mb. The radioactive of Po^{209} is 102 year and of Po^{208} is 2.90 year and of Po^{206} is 8.8 day.

Table 4.7. Mass number (A) cross sections obtained for isotope of ${}_{84}\text{Po}$ at reaction $p+{}_{83}\text{Bi}^{209}$; $E_p=150$ MeV energy. Calculations have been made with CEM03 and ALICE/ASH code

${}^{209}\text{Bi} (p,x) {}_{84}\text{Po}^{197-209}$; $E_p=150$ MeV			
Mass number (A)	Radioactive Half life	CEM03-Code Cross section (mb)	ALICE/ASH-Code Cross section (mb)
209	102 year (α)	21.3	13.9
208	2.90 year (α)	25.5	17.4
207		27.6	25.2
206	8.8 day (e)	29.2	27.6
205		40.6	27.3
204		40.6	33.6
203		39.0	35.7
202		48.2	
201		35.3	
200		30.8	
199		14.8	
198		12.1	
197		4.92	

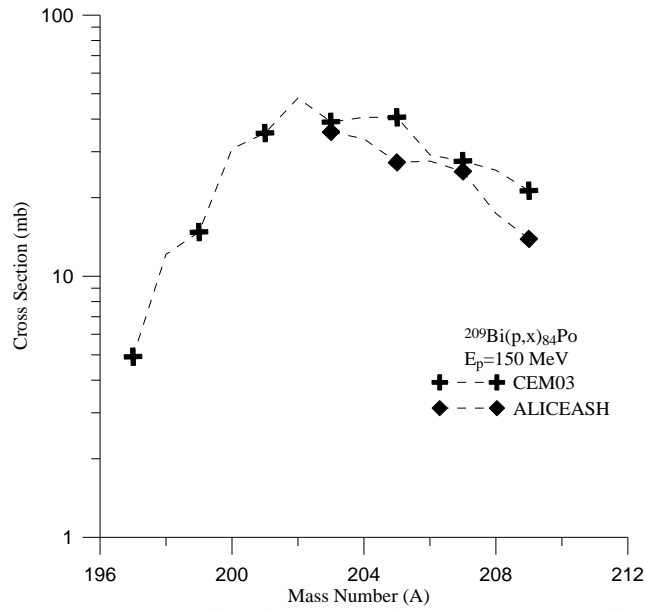


Figure 4.7. Mass number (A) cross sections obtained for isotope of ${}_{84}\text{Po}$ at reaction $p+{}_{83}\text{Bi}^{209}$; $E_p=150$ MeV energy. Calculations have been made with CEM03 and ALICE/ASH code

4.4.8. ${}_{81}\text{Tl}^{191-208}$ the product resulting from the reaction of $p+{}_{83}\text{Bi}^{209}$

The formation cross section of the ${}_{81}\text{Tl}$ isotope with the different mass number (A) have been obtained for reaction $p+{}_{83}\text{Bi}^{209}$ at energy $E_p=200$ MeV. The product resulting from the reaction of the proton at different energies has been shown in Figure 4.8. The maximum formation level of isotope Tl^{195} is 18.3 mb and the minimum formation of isotope Tl^{205} is 1.34 mb. The radioactive of Tl^{204} is 3.77 year and of Tl^{202} is 12.2 day.

Table 4.8. Mass number (A) cross sections obtained for isotope of ${}_{81}\text{Tl}$ at reaction $p+{}_{83}\text{Bi}^{209}$; $E_p=200$ MeV energy. Calculations have been made with CEM03 and ALICE/ASH code

${}^{209}\text{Bi} (p,x) {}_{81}\text{Tl}^{191-208}$; $E_p=200$ MeV			
Mass number (A)	Radioactive Half life	CEM03-Code Cross section (mb)	ALICE/ASH-Code Cross section (mb)
208			
207			
206			
205		1.34	
204	3.77 year (β)	2.85	
203		4.03	0.10
202	12.2 day (e)	5.71	0.33
201		7.05	0.66
200		8.06	0.64
199		13.4	
198		13.4	
197		13.6	
196		11.4	
195		18.3	
194		10.9	
193		8.06	
192		4.36	
191		3.02	

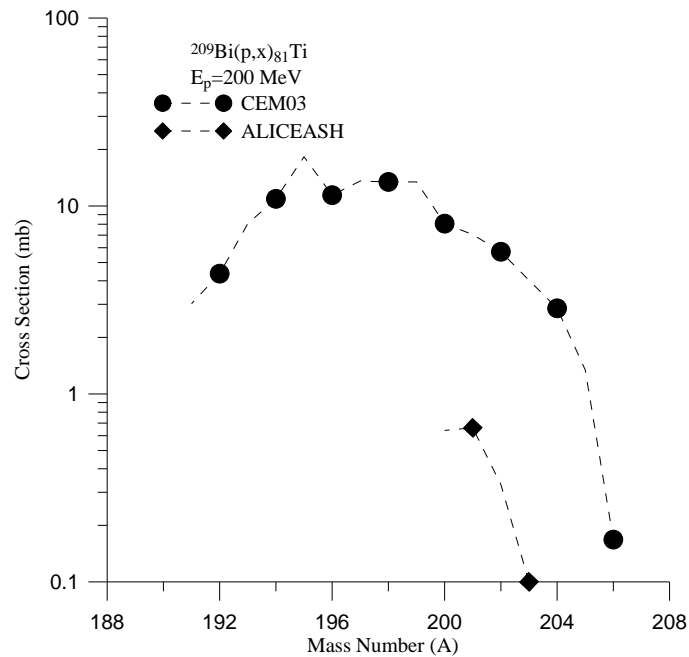


Figure 4.8. Mass number (A) cross sections obtained for isotope of ${}_{81}\text{Tl}$ at reaction $p+{}_{83}\text{Bi}^{209}$; $E_p=200$ MeV energy. Calculations have been made with CEM03 and ALICE/ASH code

4.4.9. ${}_{82}\text{Pb}^{192-208}$ the product resulting from the reaction of $\text{p}+{}_{83}\text{Bi}^{209}$

The formation cross sections of the ${}_{82}\text{Pb}$ isotopes with the different mass number (A) have been obtained for reaction $\text{p}+{}_{83}\text{Bi}^{209}$ at energy $E_p=200$ MeV. The product resulting from the reaction of the proton at different energies has been shown in Figure 4.9. The maximum formation level of isotope Pb^{198} is 47.7 mb and the minimum formation level of isotope Pb^{208} is 2.18 mb. The radioactive of Pb^{205} is 15 M year and of Pb^{202} is 0.05 M year.

Table 4.9. Mass number (A) cross sections obtained for isotope of ${}_{82}\text{Pb}$ at reaction $\text{p}+{}_{83}\text{Bi}^{209}$; $E_p=200$ MeV energy. Calculations have been made with CEM03 and ALICE/ASH code

${}^{209}\text{Bi}(\text{p},\text{x}){}_{82}\text{Pb}^{192-208}$; $E_p=200$ MeV			
Mass number (A)	Radioactive Half life	CEM03-Code Cross section (mb)	ALICE/ASH-Code Cross section (mb)
208		2.18	25.9
207		19.1	25
206		25.8	29.8
205	15 M year (e)	22.0	27.2
204		29.0	27
203		24.5	33.4
202	0.05 M year (e)	39.1	42.4
201		33.1	37.8
200		39.4	
199		33.1	
198		47.7	
197		38.4	
196		43.1	
195		23.3	
194		16.6	
193		7.05	
192		2.18	

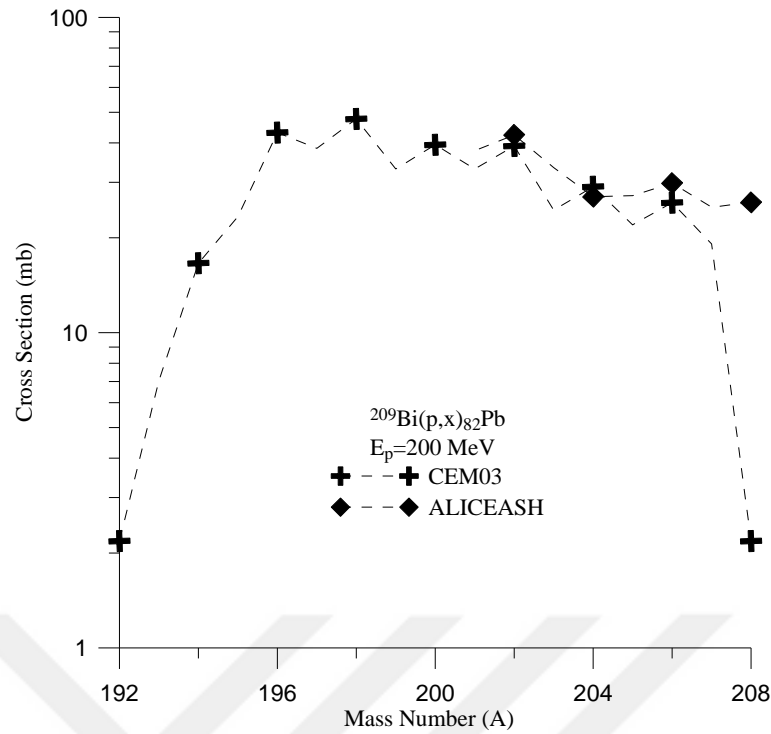


Figure 4.9. Mass number (A) cross sections obtained for isotope of ${}_{82}\text{Pb}$ at reaction $p+{}_{83}\text{Bi}^{209}$; $E_p=200$ MeV energy. Calculations have been made with CEM03 and ALICE/ASH code

4.4.10. ${}_{84}\text{Po}^{195-209}$ the product resulting from the reaction of $p+{}_{83}\text{Bi}^{209}$

The formation cross section of the ${}_{84}\text{Po}$ isotope with the different mass number (A) have been obtained for reaction $p+{}_{83}\text{Bi}^{209}$ at energy $E_p=200$ MeV energy. The product resulting from the reaction of the proton at different energies has been shown in Figure 4.10. The maximum formation level of isotope Po^{204} is 28.9 mb and the minimum formation level of isotope Po^{195} is 2.18 mb. The radioactive of Po^{209} is 102 year of Po^{208} is 2.90 year and of Po^{206} is 8.8 day.

Table 4.10. Mass number (A) cross sections obtained for isotope of ${}_{84}\text{Po}$ at reaction $p+{}_{83}\text{Bi}^{209}$; $E_p=200$ MeV energy. Calculations have been made with CEM03 and ALICE/ASH code

${}^{209}\text{Bi} (p,x) {}_{84}\text{Po}^{195-209}$; $E_p=200$ MeV			
Mass number (A)	Radioactive Half life	CEM03-Code Cross section (mb)	ALICE/ASH-Code Cross section (mb)
209	102 year (α)	14.6	10.9
208	2.90 year (α)	21.7	10.6
207		20.6	15
206	8.8 day (e)	26.9	12.2
205		26.0	16.8
204		28.9	13.3
203		23.5	15.8
202		25.8	
201		24.2	
200		25.7	
199		13.6	
198		9.57	
197		6.21	
196		4.87	
195		2.18	

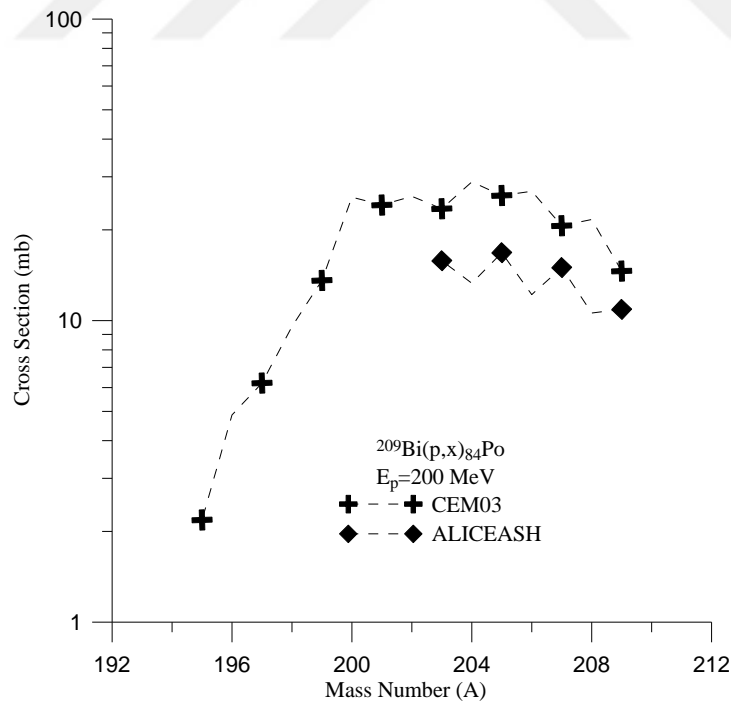


Figure 4.10. Mass number (A) cross sections obtained for isotope of ${}_{84}\text{Po}$ at reaction $p+{}_{83}\text{Bi}^{209}$; $E_p=200$ MeV energy. Calculations have been made with CEM03 and ALICE/ASH code

4.4.11. ${}_{82}\text{Pb}^{192-208}$ the product resulting from the reaction of $\text{p}+{}_{83}\text{Bi}^{209}$

The formation cross section of the ${}_{82}\text{Pb}$ isotope with the different mass number (A) have been obtained for reaction $\text{p}+{}_{83}\text{Bi}^{209}$ at energy $E_p=200$ MeV. The product resulting from the reaction of the proton at different energies has been shown in Figure 4.11. The maximum formation level of isotope Pb^{198} is 47.7 mb and the minimum formation level of isotope Pb^{208} is 2.18 mb. The radioactive of Pb^{205} is 15 M year and of Pb^{202} is 0.05 M year.

Table 4.11. Mass number (A) cross sections obtained for isotope of ${}_{82}\text{Pb}$ at reaction $\text{p}+{}_{83}\text{Bi}^{209}$; $E_p=200$ MeV energy. Calculations have been made with CEM03 and ALICE/ASH code

${}^{209}\text{Bi}(\text{p},\text{x}){}_{82}\text{Pb}^{192-208}$; $E_p=200$ MeV			
Mass number (A)	Radioactive Half life	CEM03-Code Cross section (mb)	ALICE/ASH-Code Cross section (mb)
208		2.18	25.9
207		19.1	25
206		25.8	29.8
205	15 M year (e)	22.0	27.2
204		29.0	27
203		24.5	33.4
202	0.05 M year (e)	39.1	42.4
201		33.1	37.8
200		39.4	
199		33.1	
198		47.7	
197		38.4	
196		43.1	
195		23.3	
194		16.6	
193		7.05	
192		2.18	

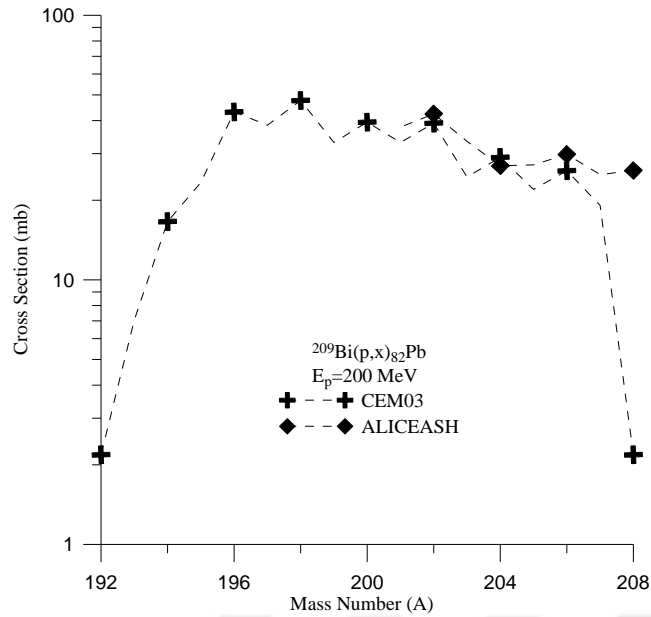


Figure 4.11. Mass number (A) cross sections obtained for isotope of ${}_{82}\text{Pb}$ at reaction $p+{}_{83}\text{Bi}^{209}$; $E_p=200$ MeV energy. Calculations have been made with CEM03 and ALICE/ASH code

4.4.12. ${}_{84}\text{Po}^{195-209}$ the product resulting from the reaction of $p+{}_{83}\text{Bi}^{209}$

The formation cross section of the ${}_{84}\text{Po}$ isotope with the different mass number (A) have been obtained for reaction $p+{}_{83}\text{Bi}^{209}$ at energy $E_p=200$ MeV. The product resulting from the reaction of the proton at different energies has been shown in Figure 4.12. The maximum formation level of isotope Po^{204} is 28.9 mb and the minimum formation level of isotope Po^{195} is 2.18 mb. The radioactive of Po^{209} is 102 year of Po^{208} is 2.90 year and of Po^{206} is 8.8 day.

Table 4.12. Mass number (A) cross sections obtained for isotope of ${}_{84}\text{Po}$ at reaction $p+{}_{83}\text{Bi}^{209}$; $E_p=200$ MeV energy. Calculations have been made with CEM03 and ALICE/ASH code

${}^{209}\text{Bi}(p,x){}_{84}\text{Po}^{195-209}$; $E_p=200$ MeV			
Mass number (A)	Radioactive Half life	CEM03-Code Cross section (mb)	ALICE/ASH-Code Cross section (mb)
209	102 year (α)	14.6	10.9
208	2.90 year (α)	21.7	10.6
207		20.6	15
206	8.8 day (e)	26.9	12.2
205		26.0	16.8
204		28.9	13.3
203		23.5	15.8
202		25.8	
201		24.2	
200		25.7	
199		13.6	
198		9.57	
197		6.21	
196		4.87	
195		2.18	

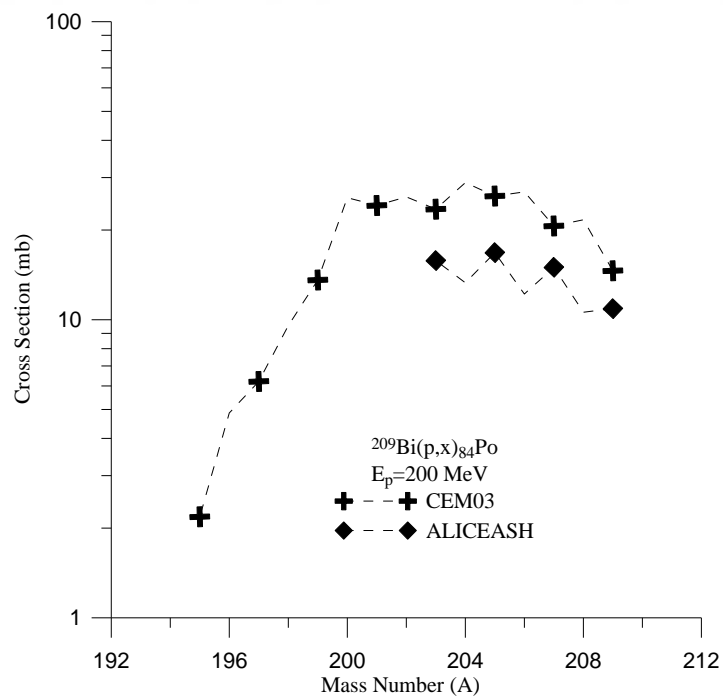


Figure 4.12. Mass number (A) cross sections obtained for isotope of ${}_{84}\text{Po}$ at reaction $p+{}_{83}\text{Bi}^{209}$; $E_p=200$ MeV energy. Calculations have been made with CEM03 and ALICE/ASH code

4.4.13. ${}_{82}\text{Pb}^{190-208}$ the product resulting from the reaction of $\text{p}+{}_{83}\text{Bi}^{209}$

The formation cross section of the ${}_{82}\text{Pb}$ isotope with the different mass number (A) have been obtained for reaction $\text{p}+{}_{83}\text{Bi}^{209}$ at energy $E_p=250$ MeV. The product resulting from the reaction of the proton at different energies has been shown in Figure 4.13. The maximum formation level of isotope Pb^{198} is 42.5 mb and the minimum formation level of isotope Pb^{190} is 1.14 mb. The radioactive of Pb^{205} is 15 M year and of Pb^{202} is 0.05 M year.

Table 4.13. Mass number (A) cross sections obtained for isotope of ${}_{82}\text{Pb}$ at reaction $\text{p}+{}_{83}\text{Bi}^{209}$; $E_p=250$ MeV energy. Calculations have been made with CEM03 and ALICE/ASH code

${}^{209}\text{Bi}(\text{p},\text{x}){}_{82}\text{Pb}^{190-208}$; $E_p=250$ MeV			
Mass number (A)	Radioactive Half life	CEM03-Code Cross section (mb)	ALICE/ASH-Code Cross section (mb)
208		1.80	23.2
207		20.6	17.5
206		27.3	23.5
205	15 M year (e)	17.2	22.6
204		25.2	23.1
203		21.6	20.1
202	0.05 M year	28.1	32.2
201		26.0	30.6
200		35.4	
199		31.7	
198		42.5	
197		37.9	
196		41.0	
195		27.9	
194		32.0	
193		16.2	
192		13.7	
191		5.39	
190		1.14	

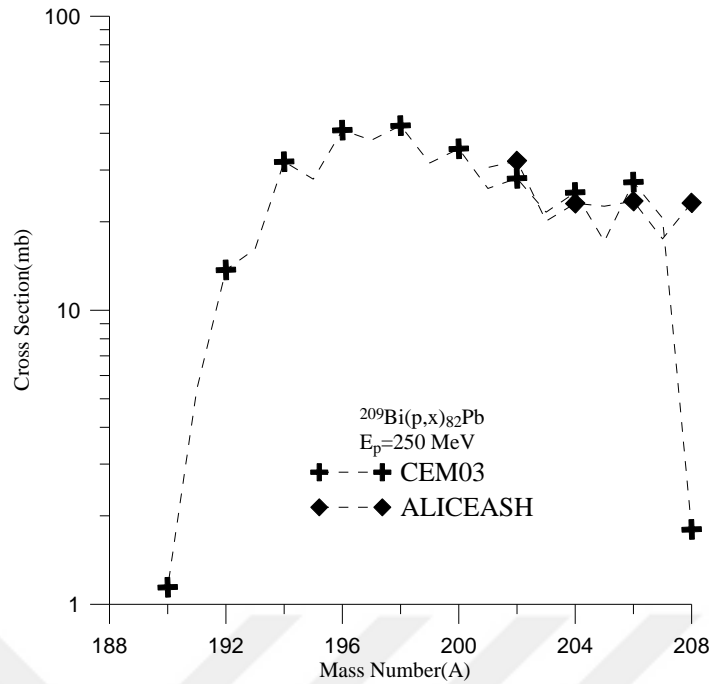


Figure 4.13. Mass number (A) cross sections obtained for isotope of ${}_{82}\text{Pb}$ at reaction $p+{}_{83}\text{Bi}^{209}$; $E_p=250$ MeV energy. Calculations have been made with CEM03 and ALICE/ASH code

4.4.14. ${}_{81}\text{Tl}^{189-208}$ the product resulting from the reaction of $p+{}_{83}\text{Bi}^{209}$

The formation cross section of the ${}_{81}\text{Tl}$ isotope with the different mass number (A) have been obtained for reaction $p+{}_{83}\text{Bi}^{209}$ at energy $E_p=250$ MeV. The product resulting from the reaction of the proton at different energies has been shown in Figure 4.14. The maximum formation level of isotope Tl^{195} is 21.9 mb and the minimum formation level of isotope Tl^{205} is 1.14 mb. The radioactive of Tl^{204} is 3.77 year and of Tl^{202} is 12.2 day.

Table 4.14. Mass number (A) cross sections obtained for isotope of $_{81}\text{Tl}$ at reaction $p+_{83}\text{Bi}^{209}$; $E_p=250$ MeV energy. Calculations have been made with CEM03 and ALICE/ASH code

$^{209}\text{Bi} (p,x)_{81}\text{Tl}^{189-208}$; $E_p=250$ MeV			
Mass number (A)	Radioactive Half life	CEM03-Code Cross section (mb)	ALICE/ASH-Code Cross section (mb)
208			
207			
206			
205		1.14	
204	3.77 year (β^-)	2.45	
203		4.57	
202	12.2 day (e)	6.21	0.17
201		6.70	0.54
200		7.84	1.01
199		10.3	
198		10.9	
197		17.2	
196		13.2	
195		21.9	
194		18.3	
193		16.2	
192		8.82	
191		9.64	
190		4.57	
189		3.43	

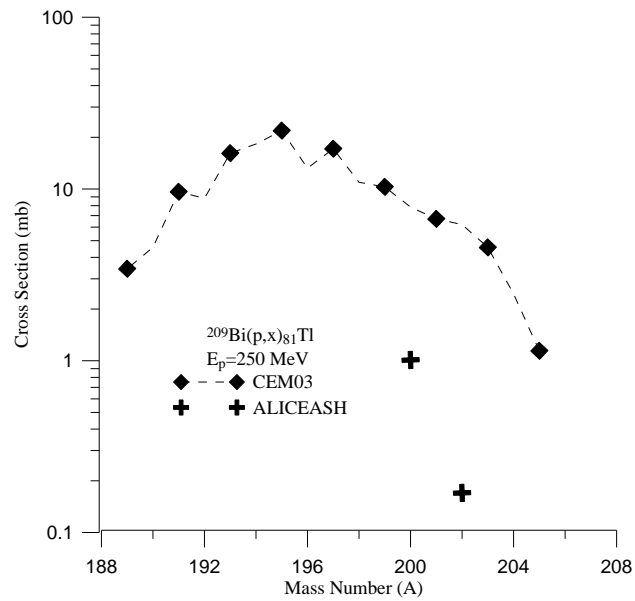


Figure 4.14. Mass number (A) cross sections obtained for isotope of $_{81}\text{Tl}$ at reaction $p+_{83}\text{Bi}^{209}$; $E_p=250$ MeV energy. Calculations have been made with CEM03 and ALICE/ASH code

4.4.15. ${}_{84}\text{Po}^{194-209}$ the product resulting from the reaction of $p+{}_{83}\text{Bi}^{209}$

The formation cross section of the ${}_{84}\text{Po}$ isotope with the different mass number (A) have been obtained for reaction $p+{}_{83}\text{Bi}^{209}$ at energy $E_p=250$ MeV. The product resulting from the reaction of the proton at different energies has been shown in Figure 4.15. The maximum formation level of isotope Po^{206} is 22.7 mb and the minimum formation level of isotope Po^{195} is 1.14 mb. The radioactive of Po^{209} is 102 year of Po^{208} is 2.90 year and of Po^{206} is 8.8 day.

Table 4.15. Mass number (A) cross sections obtained for isotope of ${}_{84}\text{Po}$ at reaction $p+{}_{83}\text{Bi}^{209}$; $E_p=250$ MeV energy. Calculations have been made with CEM03 and ALICE/ASH code

${}^{209}\text{Bi} (p,x) {}_{84}\text{Po}^{194-209}$; $E_p=250$ MeV			
Mass number (A)	Radioactive Half life	CEM03-Code Cross section (mb)	ALICE/ASH-Code Cross section (mb)
209	102 year (α)	10.8	6.19
208	2.90 year (α)	20.7	6.15
207		17.5	7.07
206	8.8 day (e)	22.7	8.8
205		17.5	10.1
204		22.7	8.01
203		18.1	8.39
202		21.9	
201		13.9	
200		15.2	
199		9.96	
198		11.8	
197		3.92	
196		5.06	
195		1.14	
194		1.14	

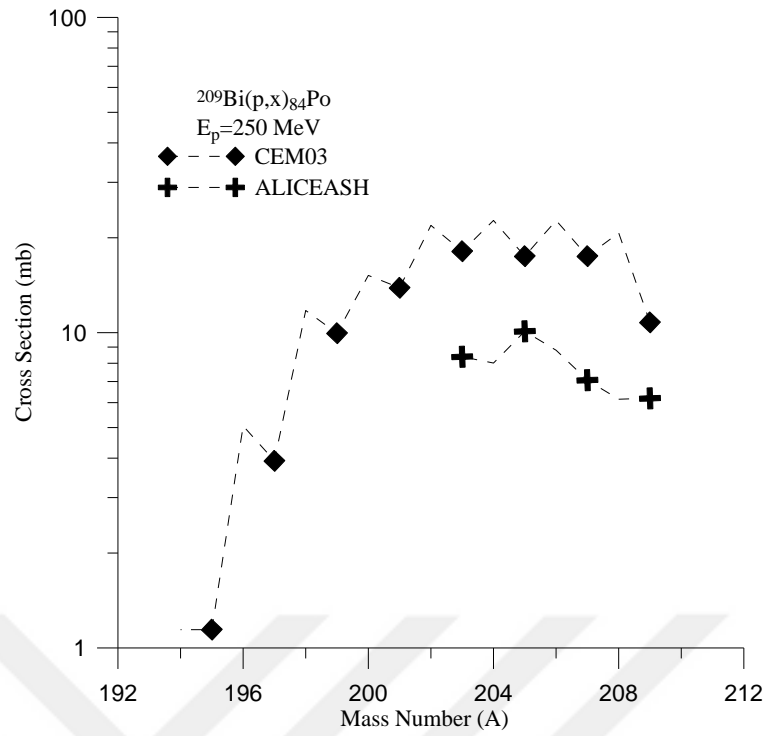


Figure 4.15. Mass number (A) cross sections obtained for isotope of $_{84}\text{Po}$ at reaction $p+_{83}\text{Bi}^{209}$; $E_p=250\text{ MeV}$ energy. Calculations have been made with CEM03 and ALICE/ASH code

4.5. $p+ {}_{74}\text{W}^{184}$ Reaction

Tungsten (W): In the rough form of tungsten, it is a grey steel metal that is often fragile and difficult to operate, it can be done easily. It is done by fraud or drawing. Of all metals in their pure form, tungsten has the highest melting point (3422 ° C, 6192 ° F), the lowest steam pressure (at temperatures above 1650 ° C, 3000 ° F) and the highest tensile strength. Tungsten has the least thermal expansion factor of any pure metal. Thermal expansion, low melting point, and high tungsten strength the strong covalent bond between the atoms are made up of the 5 D tungsten electrons. Casting small amounts of tungsten with steel greatly increases its strength.

Tungsten and its alloys, thin wires in electric bulbs, electrons and television tubes, windings and heating elements in electric ovens are used. X-ray targets, air transport, and metal evaporation it is also used in high-temperature applications. Tungsten powder, electronic there is a wide use in the industry. Tungsten carbide, metal working, mining and is an important compound in the petroleum industry.

4.5.1. ${}_{75}\text{Re}^{179-185}$ the product resulting from the reaction of $p+{}_{74}\text{W}^{184}$

The formation cross section of the ${}_{75}\text{Re}$ isotope with the different mass number (A) have been obtained for reaction $p+ {}_{74}\text{W}^{184}$ at energy $E_p=50$ MeV. The product resulting from the reaction of the proton at different energies has been shown in Figure 4.16. The maximum formation level of isotope Re^{182} is 98.78 mb and the minimum formation level of isotope Re^{179} is 12.21 mb. The radioactive of Re^{184} is 71 day and of Re^{183} is 38 day.

Table 4.16. Mass number (A) cross sections obtained for isotope of ${}_{75}\text{Re}$ at reaction $p+ {}_{74}\text{W}^{184}$; $E_p=50$ MeV energy. Calculations have been made with CEM03 and ALICE/ASH and PCROS code

${}^{184}\text{W} (p,x) {}_{75}\text{Re}^{179-185}$; $E_p=50$ MeV				
Mass number (A)	Radioactive Half life	CEM03-Code Cross section (mb)	ALICE/ASH-Code Cross section (mb)	PCROS (mb)
185		0	0	1.95421
184	38 day (e)	31.9	41.1	
183	71 day (e)	83.01	79.3	
182		98.78	123	
181		22.87	266	
180		55.89	620	
179		12.21	118	

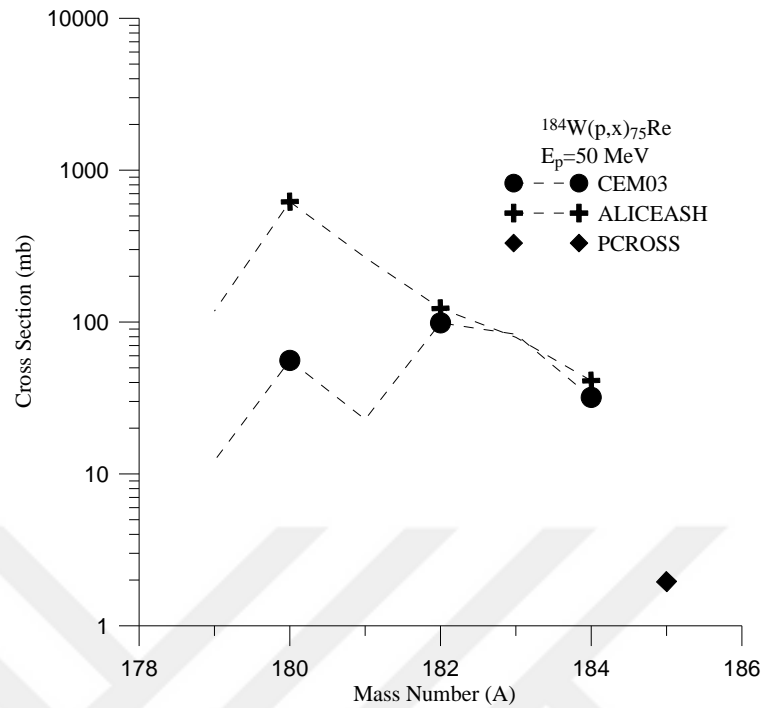


Figure 4.16. Mass number (A) cross sections obtained for isotope of ${}_{75}\text{Re}$ at reaction $p+{}_{74}\text{W}^{184}$; $E_p=50$ MeV energy. Calculations have been made with CEM03 and ALICE/ASH and PCROSS code

4.5.2. ${}_{74}\text{W}^{179-184}$ the product resulting from the reaction of $p+{}_{74}\text{W}^{184}$

The formation cross section of the ${}_{74}\text{W}$ isotope with the different mass number (A) have been obtained for reaction $p+{}_{74}\text{W}^{184}$ at energy $E_p=50$ MeV. The product resulting from the reaction of the proton at different energies has been shown in Figure 4.17. The maximum formation level of isotope W^{182} is 201.8 mb and the minimum formation level of isotope W^{184} is 50.91 mb. The radioactive of W^{181} is 121 day.

Table 4.17. Mass number (A) cross sections obtained for isotope of ${}_{74}\text{W}$ at reaction $p+{}_{74}\text{W}^{184}$; $E_p=50$ MeV energy. Calculations have been made with CEM03 and ALICE/ASH and PCROS code

${}^{184}\text{W} (p,x) {}_{74}\text{W}$; $E_p=50$ MeV				
Mass number (A)	Radioactive Half life	CEM03-Code Cross section (mb)	ALICE/ASH-Code Cross section (mb)	PCROS (mb)
184		50.91	39.3	471.504
183		126	120	
182		201.8	199	
181	121 day (e)	179.7	188	
180		115.5	38.3	
179		8.117		

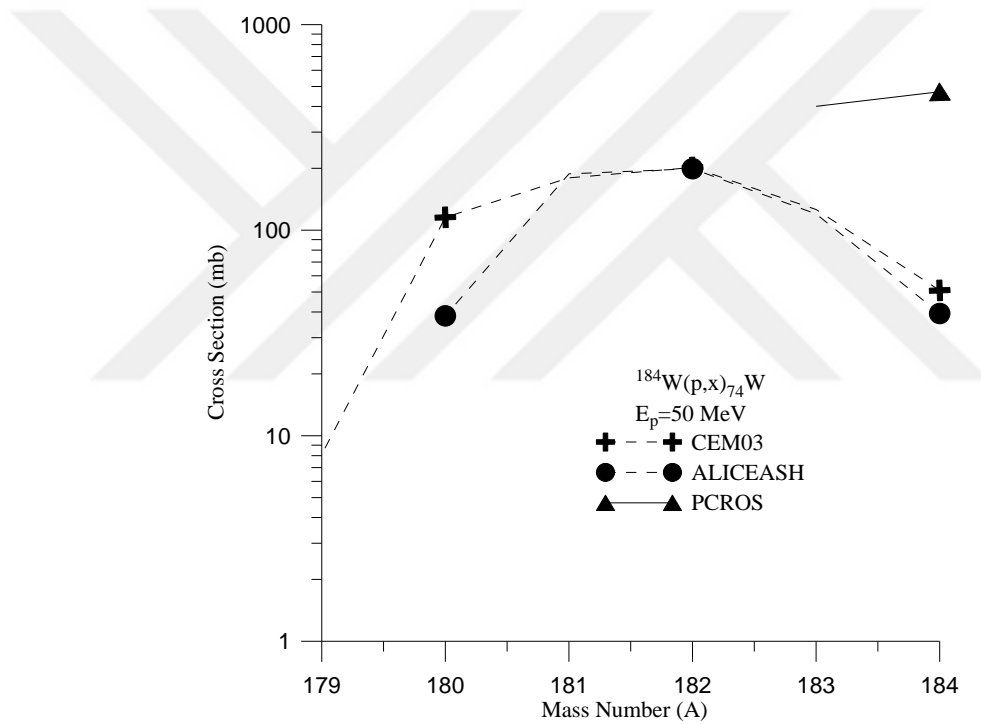


Figure 4.17. Mass number (A) cross sections obtained for isotope of ${}_{74}\text{W}$ at reaction $p+{}_{74}\text{W}^{184}$; $E_p=50$ MeV energy. Calculations have been made with CEM03 and ALICE/ASH and PCROS code

4.5.3. ${}_{73}\text{Ta}^{173-183}$ the product resulting from the reaction of $p+{}_{74}\text{W}^{184}$

The formation cross section of the ${}_{73}\text{Ta}$ isotope with the different mass number (A) have been obtained for reaction $p+{}_{74}\text{W}^{184}$ at energy $E_p=100$ MeV. The product resulting from the reaction of the proton at different energies has been shown in Figure 4.18. The maximum formation level of isotope Ta^{175} is 85 mb and the minimum formation level of isotope Pb^{183}

is 5.90 mb. The radioactive of Ta¹⁸³ is 665 day and of Ta¹⁸² is 115 day and of Ta¹⁷⁹ is 5.1 day.

Table 4.18. Mass number (A) cross sections obtained for isotope of ⁷³Ta at reaction p+ ¹⁸⁴W¹⁸⁴; E_p=100 MeV energy. Calculations have been made with CEM03 and ALICE/ASH code

¹⁸⁴ W (p,x) ⁷³ Ta ¹⁷³⁻¹⁸³ ; E _p =100 MeV			
Mass number (A)	Radioactive Half life	CEM03-Code Cross section (mb)	ALICE/ASH-Code Cross section (mb)
183	5.1 day (β ⁻)	5.90	25.8
182	115 day (β ⁻)	16.0	25.4
181		32.4	31.7
180		28.6	36.9
179	665 day (e)	35.0	23.3
178		36.1	7.54
177		28.6	7.78
176		12.3	1.94
175		85.0	
174		57.2	
173		83.2	

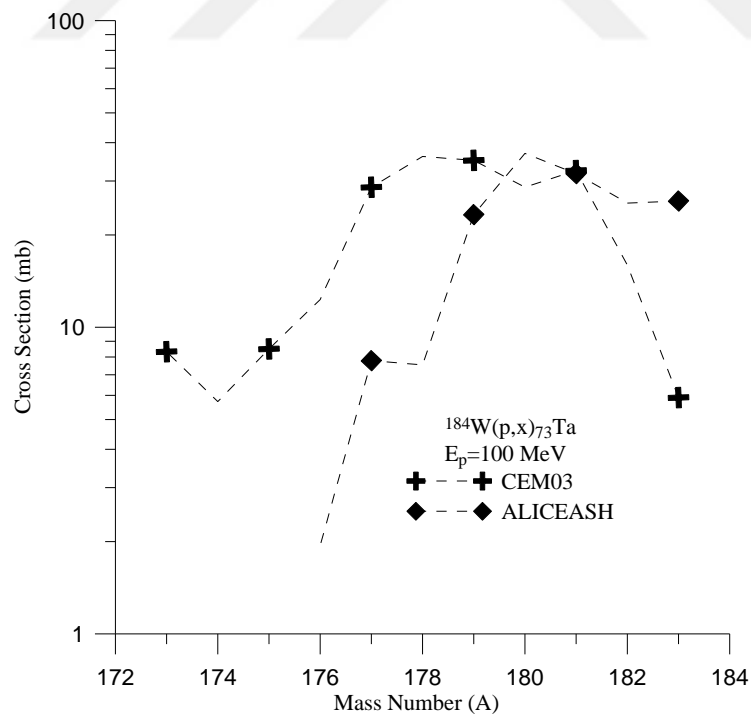


Figure 4.18. Mass number (A) cross sections obtained for isotope of ⁷³Ta at reaction p+ ¹⁸⁴W¹⁸⁴; E_p=100 MeV energy. Calculations have been made with CEM03 and ALICE/ASH code

4.5.4. ${}_{75}\text{Re}^{175-184}$ the product resulting from the reaction of $p+{}_{74}\text{W}^{184}$

The formation cross section of the ${}_{75}\text{Re}$ isotope with the different mass number (A) have been obtained for reaction $p+{}_{74}\text{W}^{184}$ at energy $E_p=100$ MeV. The product resulting from the reaction of the proton at different energies has been shown in Figure 4.19. The maximum formation level of isotope Re^{179} is 80.6 mb and the minimum formation level of isotope Re^{184} is 21.9 mb. The radioactive of Re^{184} is 71 day and of Re^{183} is 38 day.

Table 4.19. Mass number (A) cross sections obtained for isotope of ${}_{75}\text{Re}$ at reaction $p+{}_{74}\text{W}^{184}$; $E_p=100$ MeV energy. Calculations have been made with CEM03 and ALICE/ASH code

${}^{184}\text{W} (p,x) {}_{75}\text{Re}^{175-184} E_p=100$ MeV			
Mass number (A)	Radioactive Half life	CEM03-Code Cross section (mb)	ALICE/ASH-Code Cross section (mb)
184	38 day (e)	21.9	24
183	71 day (e)	41.4	33.6
182		42.8	48.1
181		64.3	55.5
180		60.3	61.1
179		80.6	88.9
178		60.7	110
177		76.3	
176		69.4	
175		33.3	

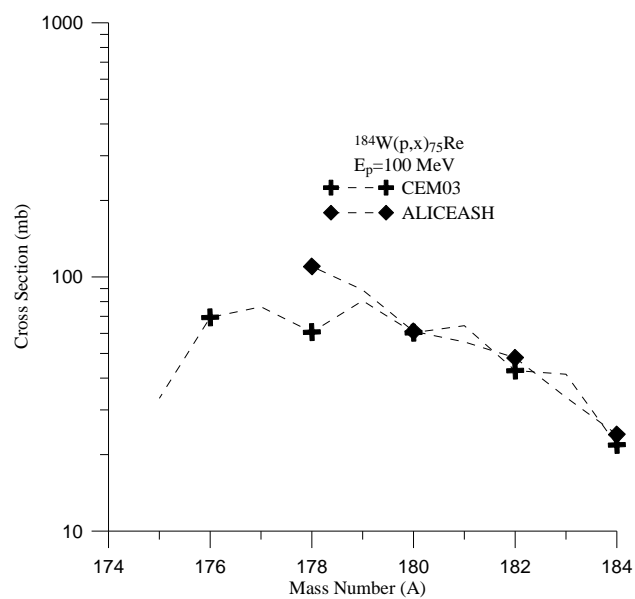


Figure 4.19. Mass number (A) cross sections obtained for isotope of ${}_{75}\text{Re}$ at reaction $p+{}_{74}\text{W}^{184}$; $E_p=100$ MeV energy. Calculations have been made with CEM03 and ALICE/ASH code

4.5.5. ${}_{72}\text{Hf}^{169-180}$ the product resulting from the reaction of $p+{}_{74}\text{W}^{184}$

The formation cross section of the ${}_{72}\text{Hf}$ isotope with the different mass number (A) have been obtained for reaction $p+{}_{74}\text{W}^{184}$ at energy $E_p=150$ MeV. The product resulting from the reaction of the proton at different energies has been shown in Figure 4.20. The maximum formation level of isotope Hf^{174} is 11.8 mb and the minimum formation level of isotope Hf^{180} is 1.29 mb. The radioactive of Hf^{175} is 70 day.

Table 4.20. Mass number (A) cross sections obtained for isotope of ${}_{72}\text{Hf}$ at reaction $p+{}_{74}\text{W}^{184}$; $E_p=150$ MeV energy. Calculations have been made with CEM03 and ALICE/ASH code

${}^{184}\text{W} (p,x) {}_{72}\text{Hf}^{169-180}$; $E_p=150$ MeV			
Mass number (A)	Radioactive Half life	CEM03-Code Cross section (mb)	ALICE/ASH-Code Cross section (mb)
180		1.29	
179		2.58	0.12
178		6.61	0.68
177		4.84	0.42
176		10.2	0.23
175	70 day (e)	10.2	0.53
174		11.8	
173		9.51	
172		8.54	
171		5.16	
170		4.35	
169		1.77	

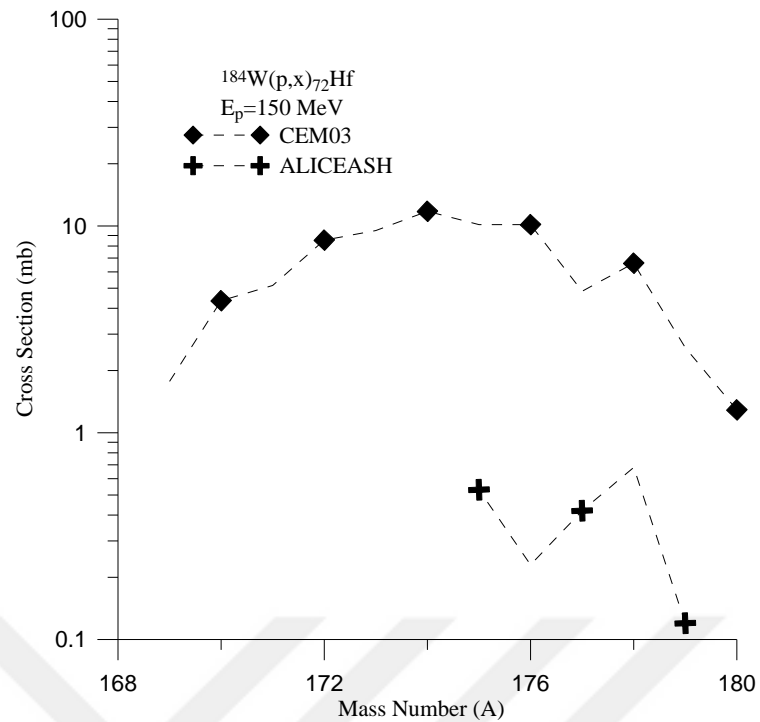


Figure 4.20. Mass number (A) cross sections obtained for isotope of ${}_{72}\text{Hf}$ at reaction $p+{}_{74}\text{W}^{184}$; $E_p=150$ MeV energy. Calculations have been made with CEM03 and ALICE/ASH code

4.5.6. ${}_{73}\text{Ta}^{169-183}$ the product resulting from the reaction of $p+{}_{74}\text{W}^{184}$

The formation cross section of the ${}_{73}\text{Ta}$ isotope with the different mass number (A) have been obtained for reaction $p+{}_{74}\text{W}^{184}$ at energy $E_p=150$ MeV. The product resulting from the reaction of the proton at different energies has been shown in Figure 4.21. The maximum formation level of isotope Ta^{175} is 54.2 mb and the minimum formation level of isotope Ta^{183} is 3.06 mb. The radioactive of Ta^{183} is 115 day of Ta^{182} is 665 day and of Ta^{179} is 5.1 day.

Table 4.21. Mass number (A) cross sections obtained for isotope of ${}_{73}\text{Ta}$ at reaction $p+{}_{74}\text{W}^{184}$; $E_p=150$ MeV energy. Calculations have been made with CEM03 and ALICE/ASH code

${}^{184}\text{W} (p,x) {}_{73}\text{Ta}^{169-183}$; $E_p=150$ MeV			
Mass number (A)	Radioactive Half life	CEM03-Code Cross section (mb)	ALICE/ASH-Code Cross section (mb)
183	5.1 day (β^-)	3.06	28.5
182	115 day (β^-)	12.7	22.1
181		27.6	27.2
180		25.6	33.8
179	665 day (e)	29.8	33.4
178		30.1	46.9
177		43.2	42.6
176		35.1	16.1
175		54.2	
174		32.6	
173		31.9	
172		13.5	
171		7.74	
170		5.32	
169		4.19	

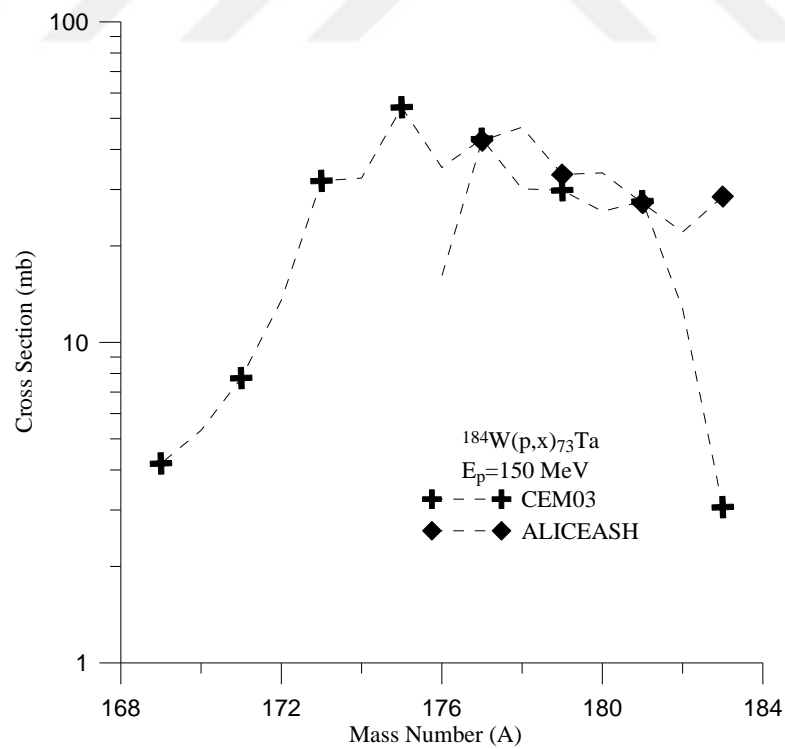


Figure 4.21. Mass number (A) cross sections obtained for isotope of ${}_{73}\text{Ta}$ at reaction $p+{}_{74}\text{W}^{184}$; $E_p=150$ MeV energy. Calculations have been made with CEM03 and ALICE/ASH code

4.5.7. ${}_{75}\text{Re}^{171-184}$ the product resulting from the reaction of $p+{}_{74}\text{W}^{184}$

The formation cross section of the ${}_{75}\text{Re}$ isotope with the different mass number (A) have been obtained for reaction $p+{}_{74}\text{W}^{184}$ at energy $E_p=150$ MeV. The product resulting from the reaction of the proton at different energies has been shown in Figure 4.22. The maximum formation level of isotope Re^{179} is 37.9 mb and the minimum formation level of isotope Re^{171} is 1.13 mb. The radioactive of Re^{184} is 71 day and of Re^{183} is 38 day.

Table 4.22. Mass number (A) cross sections obtained for isotope of ${}_{75}\text{Re}$ at reaction $p+{}_{74}\text{W}^{184}$; $E_p=150$ MeV energy. Calculations have been made with CEM03 and ALICE/ASH code

${}^{184}\text{W} (p,x) {}_{75}\text{Re}^{171-184}$; $E_p=150$ MeV			
Mass number (A)	Radioactive Half life	CEM03-Code Cross section (mb)	ALICE/ASH-Code Cross section (mb)
184	38 day (e)	12.9	12.8
183	71 day (e)	28.2	18.2
182		26.9	24.6
181		29.8	25.2
180		32.9	29.2
179		37.9	23.8
178		31.8	38
177		36.4	
176		26.1	
175		26.3	
174		17.9	
173		15.8	
172		5.16	
171		1.13	

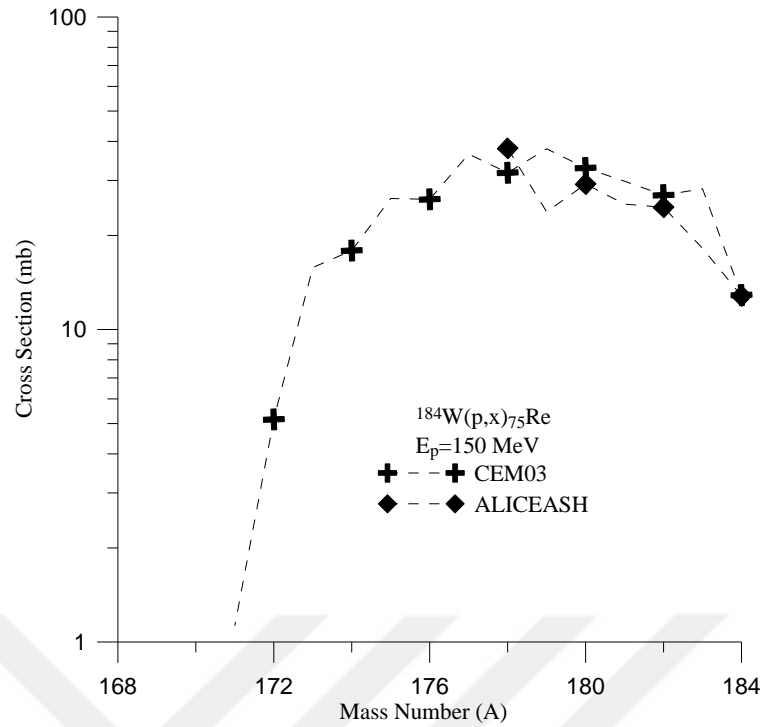


Figure 4.22. Mass number (A) cross sections obtained for isotope of ${}_{75}\text{Re}$ at reaction $p+{}_{74}\text{W}^{184}$; $E_p=150$ MeV energy. Calculations have been made with CEM03 and ALICE/ASH code

4.5.8. ${}_{72}\text{Hf}^{165-180}$ the product resulting from the reaction of $p+{}_{74}\text{W}^{184}$

The formation cross section of the ${}_{72}\text{Hf}$ isotope with the different mass number (A) have been obtained for reaction $p+{}_{74}\text{W}^{184}$ at energy $E_p=200$ MeV. The product resulting from the reaction of the proton at different energies has been shown in Figure 4.23. The maximum level of isotope Hf^{170} is 20.9 mb, and the minimum level of isotope Hf^{180} is 1.08 mb. The radioactive of Hf^{175} is 70 day.

Table 4.23. Mass number (A) cross sections obtained for isotope of ${}_{72}\text{Hf}$ at reaction $p+{}_{74}\text{W}^{184}$; $E_p=200$ MeV energy. Calculations have been made with CEM03 and ALICE/ASH code

${}^{184}\text{W} (p,x) {}_{72}\text{Hf}^{165-180}$; $E_p=200\text{MeV}$			
Mass number (A)	Radioactive Half life	CEM03-Code Cross section (mb)	ALICE/ASH-Code Cross section (mb)
180		1.08	
179		1.54	
178		3.99	0.45
177		5.68	1.8
176		9.06	2.38
175	70 day (e)	9.21	1.75
174		14.6	
173		16.9	
172		16.7	
171		15.8	
170		20.9	
169		13.1	
168		11.8	
167		6.91	
166		3.69	
165		1.23	

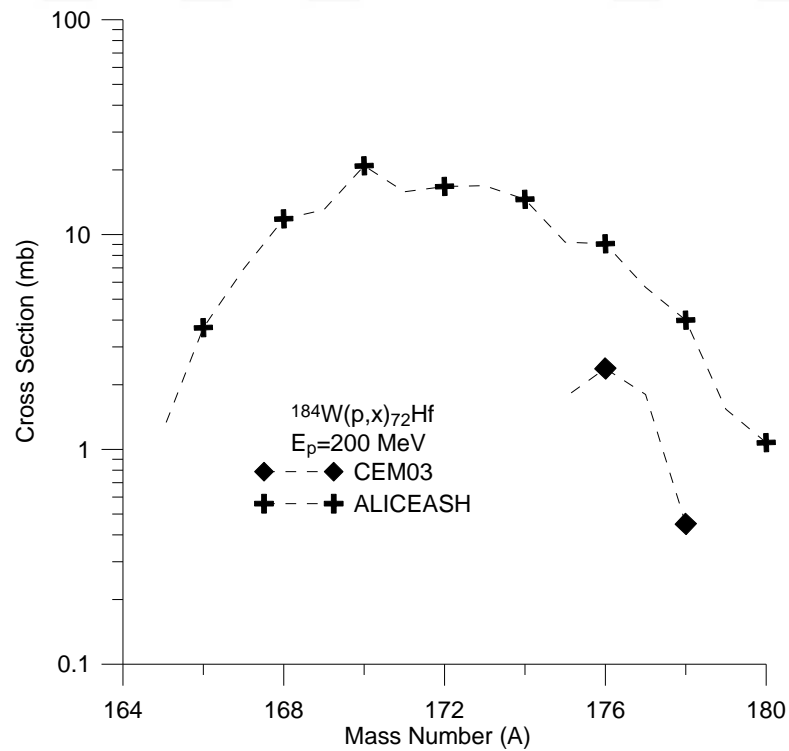


Figure 4.23. Mass number (A) cross sections obtained for isotope of ${}_{72}\text{Hf}$ at reaction $p+{}_{74}\text{W}^{184}$; $E_p=200$ MeV energy. Calculations have been made CEM03 with ALICE/ASH code

4.5.9. ${}_{73}\text{Ta}^{167-183}$ the product resulting from the reaction of $p+{}_{74}\text{W}^{184}$

The formation cross section of the ${}_{73}\text{Ta}$ isotope with the different mass number (A) have been obtained for reaction $p+{}_{74}\text{W}^{184}$ at energy $E_p=200$ MeV. The product resulting from the reaction of the proton at different energies has been shown in Figure 4.24. The maximum formation level of isotope Ta^{173} is 45.2 mb and the minimum formation level of isotope Ta^{167} is 2.61 mb. The radioactive of Ta^{183} is 115 day of Ta^{182} is 665 day and of Ta^{179} is 5.1 day.

Table 4.24. Mass number (A) cross sections obtained for isotope of ${}_{73}\text{Ta}$ at reaction $p+{}_{74}\text{W}^{184}$; $E_p=200$ MeV energy. Calculations have been made with CEM03 and ALICE/ASH code

${}^{184}\text{W} (p,x) {}_{73}\text{Ta}^{167-183}$; $E_p=200$ MeV			
Mass number (A)	Radioactive Half life	CEM03-Code Cross section (mb)	ALICE/ASH-Code Cross section (mb)
183	5.1 day (β^-)		24.4
182	115 day (β^-)	11.4	23.7
181		28.1	24.2
180		18.1	23.2
179	665 day (e)	21.8	32.1
178		21.4	44.1
177		27.3	40.2
176		25.2	56.3
175		40.1	
174		30.1	
173		45.2	
172		33.2	
171		34.6	
170		19.0	
169		14.7	
168		8.60	
167		2.61	

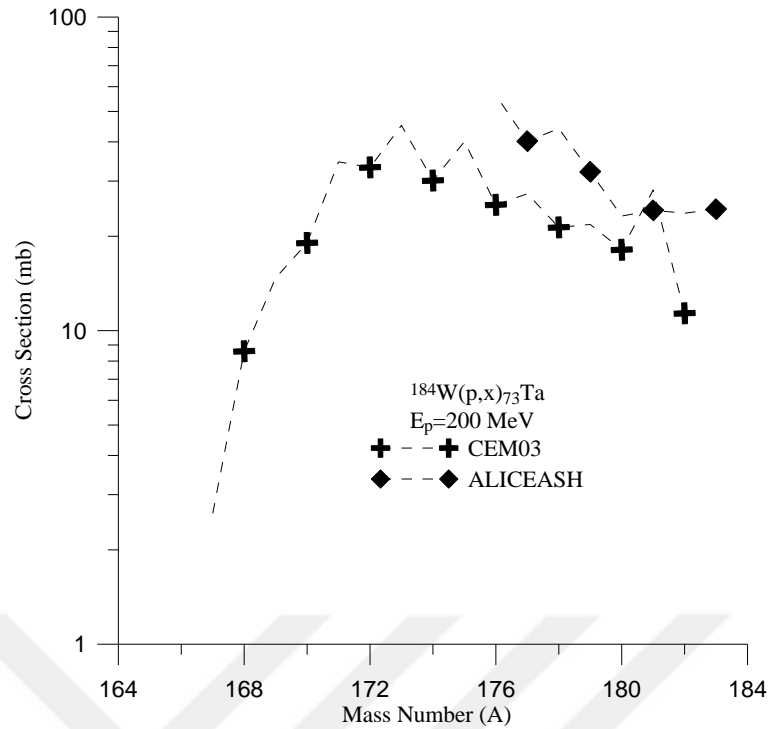


Figure 4.24. Mass number (A) cross sections obtained for isotope of ${}_{73}\text{Ta}$ at reaction $p+{}_{74}\text{W}^{184}$; $E_p=200$ MeV energy. Calculations have been made with CEM03 and ALICE/ASH code

4.5.10. ${}_{75}\text{Re}^{171-184}$ the product resulting from the reaction of $p+{}_{74}\text{W}^{184}$

The formation cross section on of the ${}_{75}\text{Re}$ isotope with the different mass number (A) have been obtained for reaction $p+{}_{74}\text{W}^{184}$ at energy $E_p=200$ MeV. The product resulting from the reaction of the proton at different energies has been shown in Figure 4.25. The maximum formation level of isotope Re^{179} is 25.8 mb and the minimum formation level of isotope Re^{171} is 3.07 (mb). The radioactive of Re^{184} is 71 day and of Re^{183} is 38 day.

Table 4.25. Mass number (A) cross sections obtained for isotope of ${}_{75}\text{Re}$ at reaction $p+{}_{74}\text{W}^{184}$; $E_p=200$ MeV energy. Calculations have been made with CEM03 and ALICE/ASH code

${}^{184}\text{W} (p,x) {}_{75}\text{Re}^{171-184}$; $E_p=200$ MeV			
Mass number (A)	Radioactive Half life	CEM03-Code Cross section (mb)	ALICE/ASH-Code Cross section (mb)
184	38 day (e)	10.8	8.12
183	71 day (e)	24.9	10.4
182		17.4	10.7
181		20.7	12.7
180		21.2	13.9
179		25.8	14.5
178		20.9	15.9
177		24.7	
176		18.4	
175		17.4	
174		13.2	
173		10.1	
172		4.91	
171		3.07	

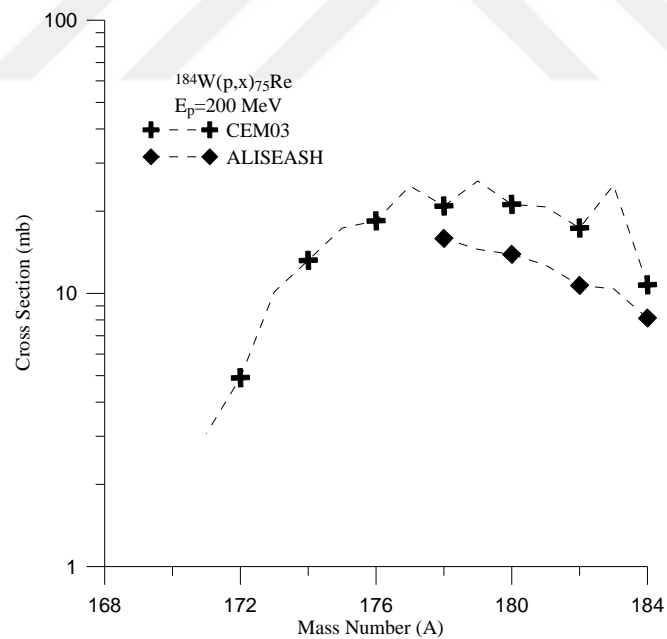


Figure 4.25. Mass number (A) cross sections obtained for isotope of ${}_{75}\text{Re}$ at reaction $p+{}_{74}\text{W}^{184}$; $E_p=200$ MeV energy. Calculations have been made with CEM03 and ALICE/ASH code

4.5.11. ${}_{72}\text{Hf}^{165-180}$ the product resulting from the reaction of $p+{}_{74}\text{W}^{184}$

The formation cross section of the ${}_{72}\text{Hf}$ isotope with the different mass number (A) have been obtained for reaction $p+{}_{74}\text{W}^{184}$ at energy $E_p=200$ MeV. The product resulting from the reaction of the proton at different energies has been shown in Figure 4.26. The maximum formation level of isotope Hf^{170} is 20.9 mb and the minimum formation of isotope Hf^{180} is 1.08 mb. The radioactive of Hf^{175} is 70 day.

Table 4.26. Mass number (A) cross sections obtained for isotope of ${}_{72}\text{Hf}$ at reaction $p+{}_{74}\text{W}^{184}$; $E_p=200$ MeV energy. Calculations have been made with CEM03 and ALICE/ASH code and experimental data

${}^{184}\text{W} (p,x) {}_{72}\text{Hf}^{165-180}$; $E_p=200$ MeV				
Mass number (A)	Radioactive Half life	CEM03-Code Cross section (mb)	ALICE/ASH-Code Cross section (mb)	EXPERIMENTAL DATA (mb)
180		1.08		
179		1.54		
178		3.99	0.45	
177		5.68	1.8	
176		9.06	2.38	
175	70 day (e)	9.21	1.75	
174		14.6		
173		16.9		
172		16.7		
171		15.8		
170		20.9		
169		13.1		
168		11.8		
167		6.91		
166		3.69		
165		1.23		6.98

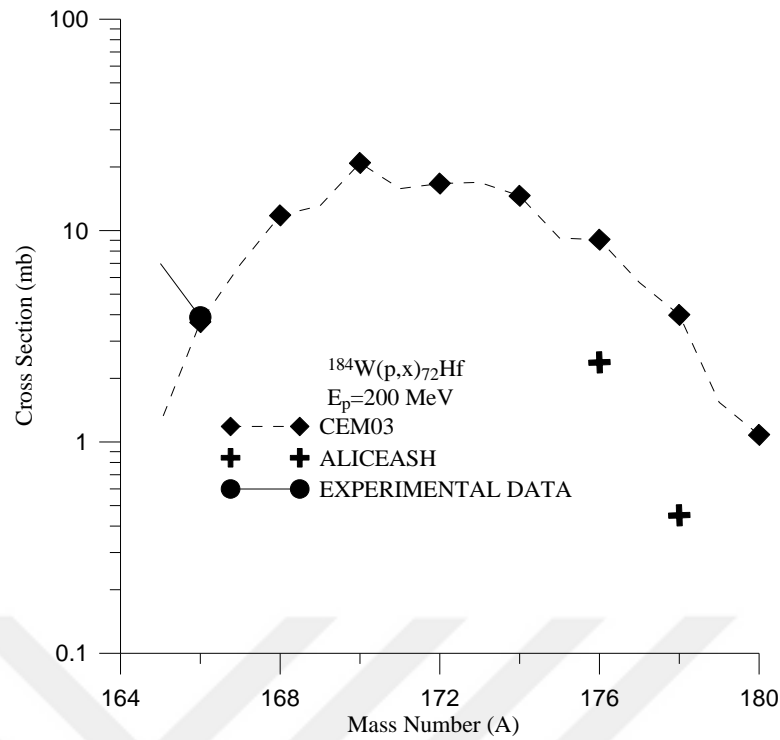


Figure 4.26. Mass number (A) cross sections obtained for isotope of ${}_{72}\text{Hf}$ at reaction $p+{}_{74}\text{W}^{184}$; $E_p=200$ MeV energy. Calculations have been made with CEM03 and ALICE/ASH code

4.5.12. ${}_{72}\text{Hf}^{163-183}$ the product resulting from the reaction of $p+{}_{74}\text{W}^{184}$

The formation cross section of the ${}_{72}\text{Hf}$ isotope with the different mass number (A) have been obtained for reaction $p+{}_{74}\text{W}^{184}$ at energy $E_p=250$ MeV. The product resulting from the reaction of the proton at different energies has been shown in Figure 4.27. The maximum formation level of isotope Hf^{168} is 24.8 mb and the minimum formation level of isotope Hf^{163} is 1.20 mb. The radioactive of Hf^{183} is 9 M year of Hf^{182} is 64 day of Hf^{181} is 42.4 day and of Hf^{175} is 70 day.

Table 4.27. Mass number (A) cross sections obtained for isotope of ${}_{72}\text{Hf}$ at reaction $p+{}_{74}\text{W}^{184}$; $E_p=250$ MeV energy. Calculations have been made with CEM03 and ALICE/ASH code

${}^{184}\text{W} (p,x) {}_{72}\text{Hf}^{163-183}$; $E_p=250$ MeV			
Mass number (A)	Radioactive Half life	CEM03-Code Cross section (mb)	ALICE/ASH-Code Cross section (mb)
183	64 day (β^-)		
182	9 M year (β^-)		
181	42.4 day (β^-)		
180		1.65	
179		1.35	
178		4.34	0.32
177		4.34	1.38
176		7.48	1.97
175	70 day (e)	7.48	3.88
174		10.2	
173		14.2	
172		18.4	
171		17.1	
170		20.8	
169		16.0	
168		24.8	
167		17.8	
166		13.0	
165		7.33	
164		4.49	
163		1.20	

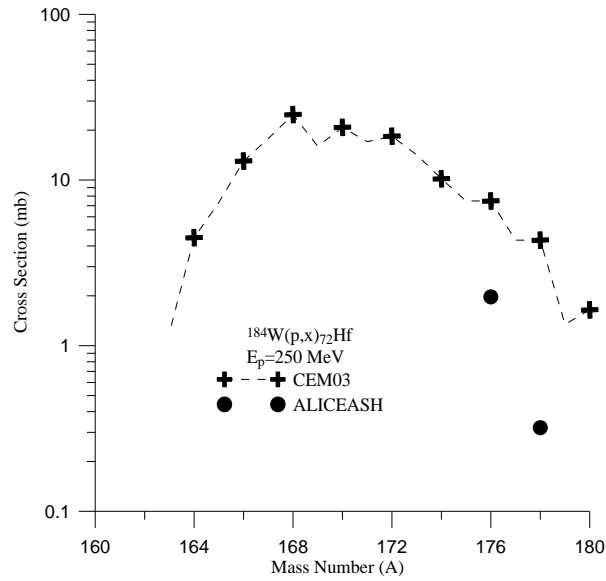


Figure 4.27. Mass number (A) cross sections obtained for isotope of ${}_{72}\text{Hf}$ at reaction $p+{}_{74}\text{W}^{184}$; $E_p=250$ MeV energy. Calculations have been made with CEM03 and ALICE/ASH code

4.5.13. ${}_{73}\text{Ta}^{165-183}$ the product resulting from the reaction of $p+{}_{74}\text{W}^{184}$

The formation cross section of the ${}_{73}\text{Ta}$ isotope with the different mass number (A) have been obtained for reaction $p+{}_{74}\text{W}^{184}$ at energy $E_p=250$ MeV. The product resulting from the reaction of the proton at different energies has been shown in Figure 4.28. The maximum formation level of isotope Ta^{175} is 33.5 mb and the minimum formation level of isotope Ta^{165} is 1.50 mb. The radioactive of Ta^{183} is 115 day of Ta^{182} is 665 day and of Ta^{179} is 5.1 day.

Table 4.28. Mass number (A) cross sections obtained for isotope of ${}_{73}\text{Ta}$ at reaction $p+{}_{74}\text{W}^{184}$; $E_p=250$ MeV energy. Calculations have been made with CEM03 and ALICE/ASH code

${}^{184}\text{W} (p,x) {}_{73}\text{Ta}^{165-183}$; $E_p=250$ MeV			
Mass number (A)	Radioactive Half life	CEM03-Code Cross section (mb)	ALICE/ASH-Code Cross section (mb)
183	5.1 day (β^-)		17.3
182	115 day (β^-)	11.4	21.4
181		30.1	20.9
180		20.0	18.1
179	665 day (e)	19.7	25.2
178		16.0	34.7
177		23.2	31.5
176		20.8	35.5
175		33.5	
174		23.5	
173		32.6	
172		25.7	
171		32.9	
170		20.9	
169		27.8	
168		17.8	
167		12.7	
166		3.44	
165		1.50	

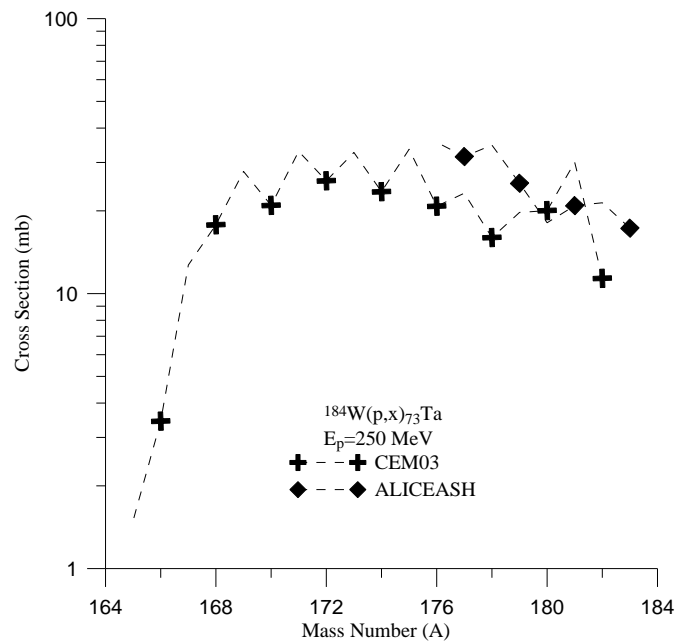


Figure 4.28. Mass number (A) cross sections obtained for isotope of ${}_{73}\text{Ta}$ at reaction $p+{}_{74}\text{W}^{184}$; $E_p=250$ MeV energy. Calculations have been made with CEM03 and ALICE/ASH code

4.5.14. ${}_{75}\text{Re}^{171-184}$ the product resulting from the reaction of $p+{}_{74}\text{W}^{184}$

The formation cross section of the ${}_{75}\text{Re}$ isotope with the different mass number (A) have been obtained for reaction $p+{}_{74}\text{W}^{184}$ at energy $E_p=250$ MeV. The product resulting from the reaction of the proton at different energies has been shown in Figure 4.29. The maximum formation level of isotope Re^{181} is 22 mb and the minimum formation level of isotope Re^{171} is 2.39 mb. The radioactive of Re^{184} is 71 day and of Re^{183} is 38 day.

Table 4.29. Mass number (A) cross sections obtained for isotope of ${}_{75}\text{Re}$ at reaction $p+{}_{74}\text{W}^{184}$; $E_p=250$ Mev energy. Calculations have been made with CEM03 and ALICE/ASH code

${}^{184}\text{W} (p,x) {}_{75}\text{Re}^{171-184}$; $E_p=250$ Mev			
Mass number (A)	Radioactive Half life	CEM03-Code Cross section (mb)	ALICE/ASH-Code Cross section (mb)
184	38 day (e)	9.42	6.05
183	71 day (e)	20.0	5.5
182		13.9	7.55
181		22.0	7.33
180		16.8	8.04
179		20.9	10
178		14.4	8.68
177		21.5	
176		12.7	
175		17.7	
174		9.27	
173		7.33	
172		3.59	
171		2.39	

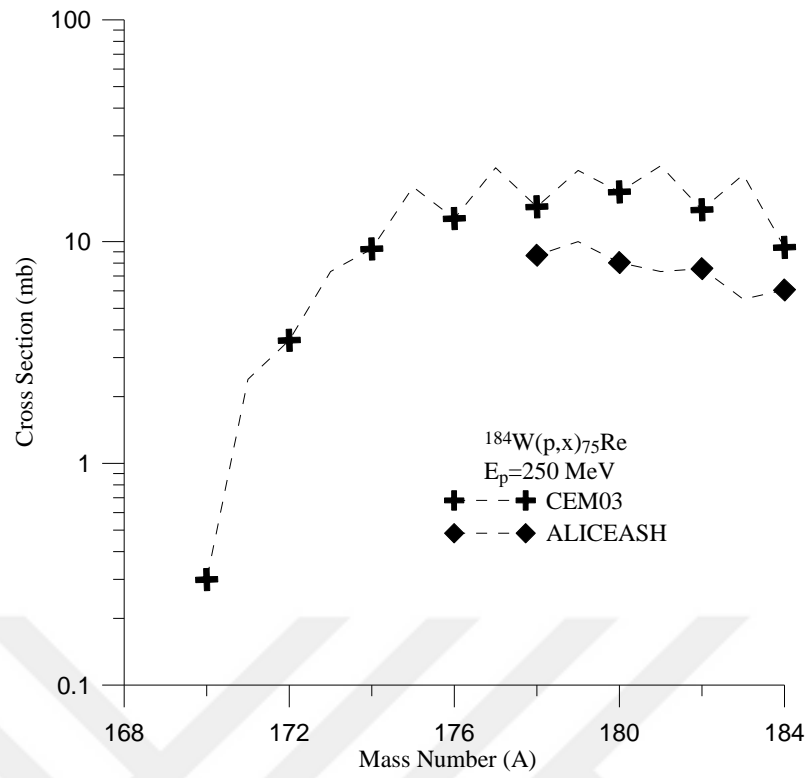


Figure 4.29. Mass number (A) cross sections obtained for isotope of ^{75}Re at reaction $p+^{184}\text{W}$; $E_p=250\text{ MeV}$ energy. Calculations have been made with CEM03 and ALICE/ASH code

5. CONCLUSION

In this study, the fragmentation production cross sections of residual nuclides in the reactions $p + {}_{74}\text{W}^{184}$ and $p + {}_{83}\text{Bi}^{209}$ has been calculated. The proton beams have 30-500 MeV energy ranges. Calculations have been made by using the Cascade Exciton Model including pre equilibrium effect and the Intra nuclear cascade model. The results of the cross sections obtained have been compared with available experimental data. Calculations have been made by using the CEM03, ALICE/ASH and PCROS codes.

Isotopes of different elements ${}_{82}\text{Pb}$, ${}_{81}\text{Ti}$, ${}_{84}\text{Po}$, ${}_{73}\text{Ta}$, ${}_{75}\text{Re}$, ${}_{72}\text{Hf}$ have been obtained at $p + {}_{74}\text{W}^{184}$, and $p + {}_{83}\text{Bi}^{209}$ reaction with protons having different energies. The reaction occurs as a result of ${}_{83}\text{Bi}^{209}$ and ${}_{74}\text{W}^{184}$ reaction with protons. The mass number (A) cross sections obtained for ${}_{82}\text{Pb}$, ${}_{81}\text{Ti}$, ${}_{84}\text{Po}$, ${}_{73}\text{Ta}$, ${}_{75}\text{Re}$, ${}_{72}\text{Hf}$ at reaction $p + {}_{83}\text{Bi}^{209}$ and $p + {}_{74}\text{W}^{184}$ for different energy of proton have been showed in the Tables⁽¹⁻²⁹⁾ and Figures⁽¹⁻²⁹⁾. Found the minimum formation level isotope of Bi^{204} is 2.937 mb at energy $E_p=50$ MeV, the maximum formation level isotope of Po^{205} is 589.4 mb at energy $E_p=50$ MeV, the maximum formation level isotope of Pb^{204} is 50.5 mb at energy $E_p=100$ MeV, the maximum formation level isotope of Ti^{199} is 10.9 mb at energy $E_p=150$ MeV, the maximum formation level isotope of Re^{182} is 98.78 mb at energy $E_p=50$ MeV, the maximum formation level isotope of W^{182} is 201.8 mb at energy $E_p=50$ MeV, the maximum formation level isotope of Ta^{175} is 85 mb at energy $E_p=100$ MeV, The maximum formation level isotope of Hf^{174} is 11.8 mb at energy $E_p=150$ MeV.

REFERENCES

Aydin A, Tel E, Şarer B (2007) Investigation of the (n, p) reaction cross-sections of some nuclei in the rare-earth elements for an incident energy range of 8–24 MeV. *Physica Scripta*, 75(3): 299

Barashenkov VS, Toneev VD (1972) Interaction of High Energy Particles and Nuclei with Atomic Nuclei (Atomizdat, in Russian 1972). RSIC CODE PACKAGE PSR-357

Benlliure J, Grewe A, De Jong M, Schmidt KH, Zhdanov S (1998) Calculated nuclide production yields in relativistic collisions of fissile nuclei. *Nuclear Physics A*, 628(3): 458-478

Bertini HW (1969) Intranuclear-cascade calculation of the secondary nucleon spectra from nucleon-nucleus interactions in the energy range 340 to 2900 MeV and comparisons with experiment. *Physical Review*, 188(4): 1711.

Bertini HW (1972) Nonelastic interactions of nucleons and π mesons with complex nuclei at energies below 3 GeV. *Physical Review C*, 6(2): 631

Blann M (1966) Evidence for the influence of shell structure on level densities in the continuum. *Nuclear Physics*, 80(1): 223-236

Blann M, Vonach, HK (1983) Global test of modified precompound decay models. *Physical Review C*, 28(4): 1475

Bohr N, Wheeler JA (1939) The mechanism of nuclear fission. *Physical Review*, 56(5): 426

Brohm T, Schmidt KH (1994) Statistical abrasion of nucleons from realistic nuclear-matter distributions. *Nuclear Physics A*, 569(4): 821-832

Chadwick B (1999) : *Nucl. Sci. Eng.* 131: 293

Cohen S, Plasil F, Swiatecki WJ (1974) Equilibrium configurations of rotating charged or gravitating liquid masses with surface tension. II. *Annals of Physics*, 82(2): 557-596

Cugnon J, Volant C, Vuillier S (1997) Nucleon and deuteron induced spallation reactions. *Nuclear Physics A*, 625(4): 729-757

De Jong M, Schmidt KH, Blank B, Böckstiegel C, Brohm T, Clerc HG, Hanelt E (1998) Fragmentation cross sections of relativistic 208Pb projectiles. *Nuclear Physics A*, 628(3): 479-492

Demirkol I (2003) Neutron Production in the Proton-Heavy Element Strike in the Design of Energy Booster. PHD, Gazi University, Institute of Science, 114

Demirkol I, Tel E, Arasoglu A, Ozmen A, Sarer B (2003) Energies 30 MeV" den 1500 Some Nuclear Spallation Reactions with Accelerated Proton up to MeV Neutron Production Influence Sections of Heavy Targets. VIII. National Nuclear Science and Technological Congress, Kayseri, Turkey

Dresner L (1962) EVAP--A Fortran Program for Calculating the Evaporation of Various Particles from Excited Compound Nuclei (No. ORNL-TM-196). Oak Ridge National Lab., Tenn

Enqvist T, Wlazlo W, Armbruster P, Benlliure J, Bernas M, Boudard A, Czajkowski S, Legrain R, Leray S, Mustapha B, Pravikoff M, Rejmund F, Schmidt KH, Stephan C, Taieb J, Tassan-Got L, Volant C (2001) Isotopic yields and kinetic energies of primary residues in 1 A GeV Pb-208+p reactions. *Nuclear Physics A*, 686(1-4): 481-524

Ericson T (1960) *Adv. Phys.* 2: 425

Ertürk S, Boztosun İ (2004) Accelerators to be used in Nuclear Physics researches and
Ertürk S, Boztosun İ (2004) Accelerators to be Used in Nuclear Physics Researches and Application Areas . II. National Congress on Particle Accelerator, Ankara, Turkey

Gabriel T, Maino G, Mashnik, SG (1994) Analysis of intermediate energy photonuclear reactions. Proc. XII Int. Sem. on High Energy Probl. Relativistic Nucl. Phys. & Quantum Chromodynamics, Dubna, Russia, 12-1

Geissel H, Münzenberg G, Riisage K (1995) Secondary Exomtic Nuclear Beams. *Annu. Rev. Nucl. Sci.* 45: 163

Gence GB (2008) Neutronic Limits on Targets with High-Energy Proton Samples. VI. YUUP Workshop, Ankara, Turkey

Gloris M, Michel R, Sudbrock F, Herpers U, Malmborg P, Holmqvist B (2001) Proton-induced production of residual radionuclides in lead at intermediate energies. *Nuclear Instruments and Methods in Physics Research Section A: Accelerators, Spectrometers, Detectors and Associated Equipment*, 463(3): 593-633

Gloris M, Michel R, Sudbrock F, Herpers U, Malmberg P, Holmqvist B (2001). Proton-induced production of residual radionuclides in lead at intermediate energies. *Nuclear Instruments and Methods in Physics Research Section A: Accelerators, Spectrometers, Detectors and Associated Equipment*, 463(3): 593-633

Gudima, Mashnik SG, Toneev VD (1983) Cascade-Exciton Model Of Nuclear Reactions. *Nuclear Physics A* 401: 329-361

Holub E, Počanić D, Čaplar R, Cindro N (1980) A consistent study of precompound and compound-nucleus emission mechanisms in neutron-induced reactions. *Zeitschrift für Physik A Atoms and Nuclei*, 296(4): 341-357

Holub E, Počanić D, Čaplar R, Cindro N (1980) A consistent study of precompound and compound-nucleus emission mechanisms in neutron-induced reactions. *Zeitschrift für Physik A Atoms and Nuclei*, 296(4): 341-357

<https://www.google.com.tr>

Iaea, Nea (2012) Uranium 2011 : Resources , Production and Demand, 488

J, JIN, 25, 1201, 1963 *Journal of Inorganic and Nuclear Chemistry*, volume 25, page 1201, 1963

Kalbach C (1975). Pre-equilibrium models in general; the Griffin model in particular. *Acta Physica Slovaca*, 25(2-3): 100-125

Kaplan A, Aydın A, Tel E, Sarer B (2009) Equilibrium and Pre-Equilibrium Emissions in Proton - Induced Reactions on ²⁰³Tl, ²⁰⁵Tl. *Pramana-Journal of Physics*, 72(2): 343- 353

Karadeniz H, Çetiner M A, Yücel H, Arkan P, Sultansoy S (2001) Accelerators Guided Reactors / Energy Booster . 1st National Particle Accelerators and Conferences of Applications and Applications, Ankara, Turkey

Koning AJ, Delaroche JP, Bersillon O (1998) Nuclear data for accelerator driven systems: Nuclear models, experiments and data libraries. *Nuclear Instruments and Methods in Physics Research Section A: Accelerators, Spectrometers, Detectors and Associated Equipment*, 414(1): 49-67

Kossov MV (2002) Approximation of photonuclear interaction cross-sections. *The European Physical Journal A-Hadrons and Nuclei*, 14(3): 377-392

Letourneau A, Galin J, Goldenbaum F, Lott B, Péghaire A, Enke M, Hilscher D, Jahnke U, Nünighoff K, Filges D, Neef R-D, Paul N, Schaal H, Sterzenbach G, Tietze A (2000) Neutron Production in Bombardments of Thin and Thick W, Hg, Pb Targets by 0.4, 0.8, 1.2, 1.8 and 2.5 GeV protons. *Nucl. Instrum. Meth. Phys. Res. B*, 170:299-322

Mashnik SG, Sierk AJ, Gudima KK, Baznat MI (2006) CEM03 and LAQGSM03-new modeling tools for nuclear applications. In Journal of Physics: Conference Series (Vol. 41, No. 1, p. 340). IOP Publishing

Millazzo-Colli L, Braga-Marcazzan GM (1974) Preformation Probability of α - Clusters in Rare earth Nuclei measured by Means of the (p, α) Reaction. Nuclear Physics A, 218: 274-284

Sarer B, Aydın A, Günay M, Korkmaz ME, Tel E (2009) Calculations of Neutron-Induced Production Cross-Sections of $^{180,182,183,184,186}\text{W}$ up to 20 MeV. Annals of Nuclear Energy, 36(4): 417-426

Sultansoy S (2001) Partial Accelerators: Yesterday, Today, Tomorrow. National Particle Accelerators and Applications Congress, Ankara, Turkey

Summerer W, Bruchle DJ, Morrissey M, Schadel B (1990) Szweryen and Yang Weifan, Physics Review. C 42: 2546

TAEK, <http://parcacikfizigi.blogspot.com/2007/11/Paracik-hospitals.html>, (Date of access:16.4.2017)

Thomas TD (1959) Cross Section for Compound-Nucleus Formation in Heavy-Ion-Induced Reactions. Physical Review, 116(3): 703

Weisskopf V (1937) Statistics and nuclear reactions. Physical Review, 52(4): 295.

Weisskopf VF, Ewing DH (1940) Phys. Rev. 57: 472

Westmacott C, Cameron R (2012) The Supply of Medical Radioisotopes. Market impacts of converting to low-enriched uranium targets for medical isotope production

Westmacott C, Cameron R (2012) The Supply of Medical Radioisotopes. Market impacts of converting to low-enriched uranium targets for medical isotope production

Wlazło W, Enqvist T, Armbruster P, Benlliure J, Bernas M, Boudard A, Pravikoff M (2000) Cross Sections of Spallation Residues Produced in 1 A GeV P 208 b on Proton Reactions. Physical review letters, 84(25): 5736

Yavas GÖ (2004) Particle Accelerators. II. National Particle Accelerators and Application Congress, Ankara, Turkey

Yildirim G (2009) Some Amphoter Group Target Nuclei in Proton Entry Reactions Reaction Cross Sections of Neutrons Produced and Their Spread Spectrum Examination. Graduate, Süleyman Demirel University, Institute of Science, Isparta, 62

Yildirim G (2009) Some Amphoter Group Target Nuclei in Proton Entry Reactions Reaction Cross Sections of Neutrons Produced and Their Spread Spectrum Examination . Graduate, Süleyman Demirel University, Institute of Science, Isparta, 62

Young GB (2008) Neutronic Limits in High Energy Proton Targeted Targets. VI. YUUP Workshop, Ankara, Turkey

R,INDC(CCP)-434,61,200302 USSR report to the I.N.D.C., number 434, page 61, 2003/02

R,ISTC-839B-99,60,2001 Internat.Science and Technology Center, Reports, number 839B-99, page 60, 2001



CURRICULUM VITAE

I was born on September 1991 in Kalar, a city of Kurdistan region of Iraq. After I completed primary, secondary and high school in Kalar, Sulaymaniyah, in 2009 I started to study physic in Sulaymaniyah university faculty of science, and graduated in 2013 holding bachelor degree of science, now I master student at Bingol University in Nuclear Physic, Bingol, Turkey.

